Source: STANDARD HANDBOOK OF ELECTRONIC ENGINEERING

CHAPTER 11.3
RADIO-FREQUENCY AMPLIFIERS AND OSCILLATORS

G. Burton Harrold, John W. Lunden, Jennifer E. Doyle, Chang S. Kim, Conrad E. Nelson, Gunter K. Wessel, Stephen W. Tehon, Y. J. Lin, Wen-Chung Wang, Harold W. Lord

RADIO-FREQUENCY AMPLIFIERS

G. Burton Harrold

Small-Signal RF Amplifiers

The prime considerations in the design of first-stage rf amplifiers are gain and noise figure. As a rule, the gain of the first rf stage should be greater than 10 dB, so that subsequent stages contribute little to the overall amplifier noise figure. The trade-off between amplifier cost and noise figure is an important design consideration. For example, if the environment in which the rf amplifier operates is noisy, it is uneconomic to demand the ultimate in noise performance. Conversely, where a direct trade-off exists in transmitter power versus amplifier noise performance, as it does in many space applications, money spent to obtain the best possible noise figure is fully justified.

Another consideration in many systems is the input-output impedance match of the rf amplifier. For example, TV cable distribution systems require an amplifier whose input and output match produce little or no line reflections. The performance of many rf amplifiers is also specified in handling large signals, to minimize cross- and intermodulation products in the output. The wide acceptance of transistors has placed an additional constraint on first-stage rf amplifiers, since many rf transistors having low noise, high gain, and high frequency response are susceptible to burnout and must be protected to prevent destruction in the presence of high-level input signals.

Another common requirement is that first rf stages be gain-controlled by automatic gain control (AGC) voltage. The amount of gain control and the linearity of control are system parameters. Many rf amplifiers have the additional requirement that they be tuned over a range of frequencies. In most receivers, regardless of configuration, local-oscillator leakage back to the input is strictly controlled by government regulation. Finally, the rf amplifier must be stable under all conditions of operation.

Device Evaluation for RF Amplifiers

An important consideration in an rf amplifier is the choice of active device. This information on device parameters can often be found in published data sheets. If parameter data are not available or not a suitable operating point, the following characterization techniques can be used.

Network Analyzers. The development of the modern network analyzer has eliminated much of the work in device and circuit evaluation. These systems automate sweep frequency measurements of the complex device or

Downloaded from Digital Engineering Library @ McGraw-Hill (www.digitalengineeringlibrary.com)
Copyright © 2004 The McGraw-Hill Companies. All rights reserved.
Any use is subject to the Terms of Use as given at the website.

RADIO-FREQUENCY AMPLIFIERS AND OSCILLATORS

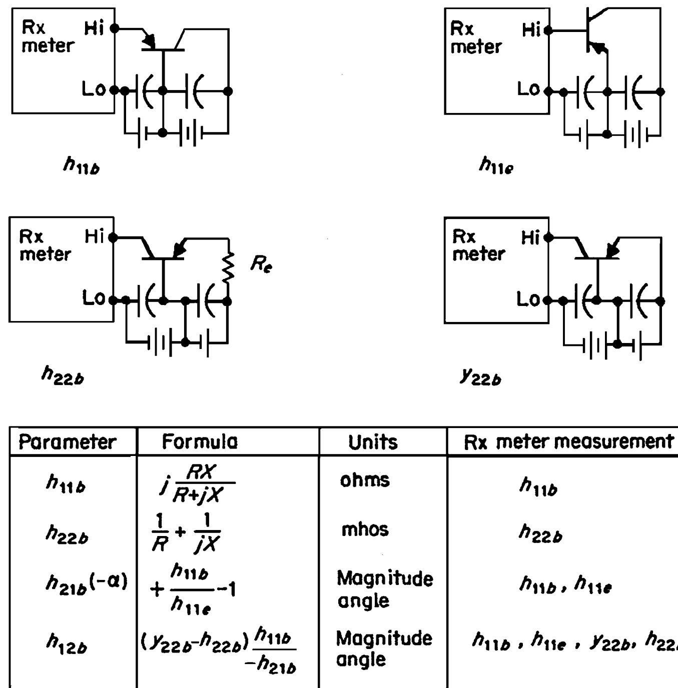

Parameter	Formula	Units	Rx meter measurement
h_{11b}	$j\frac{RX}{R+jX}$	ohms	h_{11b}
h_{22b}	$\frac{1}{R}+\frac{1}{jX}$	mhos	h_{22b}
$h_{21b}(-\alpha)$	$+\frac{h_{11b}}{h_{11e}}-1$	Magnitude angle	h_{11b}, h_{11e}
h_{12b}	$(y_{22b}-h_{22b})\frac{h_{11b}}{-h_{21b}}$	Magnitude angle	h_{11b}, h_{11e}, y_{22b}, h_{22b}

Assumes: Determinate of $|h| \ll h_{21}$ and $h_{12} \ll 1$

R and X are Rx meter's reading of parallel resistance and reactance

FIGURE 11.3.1 Use of the *Rx* meter in device characterization.

circuit parameters and avoid the tedious calculations that were previously required. The range of measurement frequencies extends from a few hertz to 60 GHz.

Network analyzers perform the modeling function by measuring the transfer and impedance function of the device by means of sine-wave excitation. These transfer voltages/currents and the reflected voltages/currents are then separated, and the proper ratios are formed to define the device parameters. There results are then displayed graphically and/or in a digital form for designer use. Newer systems allow these data to be transferred directly to computerized design programs, thus automating the total design process. The principle of actual operation is similar to that described below under *Vector Voltmeter*.

Rx Meter.* This measurement technique is usually employed at frequencies below 200 MHz for active devices that have high input and output impedance. The technique is summarized in Fig. 11.3.1 with assumptions tacit in these measurements. The biasing techniques are shown. In particular, the measurement of h_{22b} requires a very large resistor R_e to be inserted in the emitter, and this may cause difficulty in achieving the proper biasing. Care should be taken to prevent burnout of the bridge when a large dc bias is applied. The bridge's drive to the active device may be reduced for more accurate measurement by varying the B-plus voltage applied to the internal oscillator.

Vector Voltmeter.* This characterization technique measures the *S* parameters; see Fig. 11.1.9. The measurement consists in inserting the device in a transmission line, usually 50 Ω characteristic impedance, and measuring the incident and reflected voltages at the two ports of the device.

*Trademark of the Hewlett Packard Co.

Downloaded from Digital Engineering Library @ McGraw-Hill (www.digitalengineeringlibrary.com)
Copyright © 2004 The McGraw-Hill Companies. All rights reserved.
Any use is subject to the Terms of Use as given at the website.

RADIO-FREQUENCY AMPLIFIERS AND OSCILLATORS

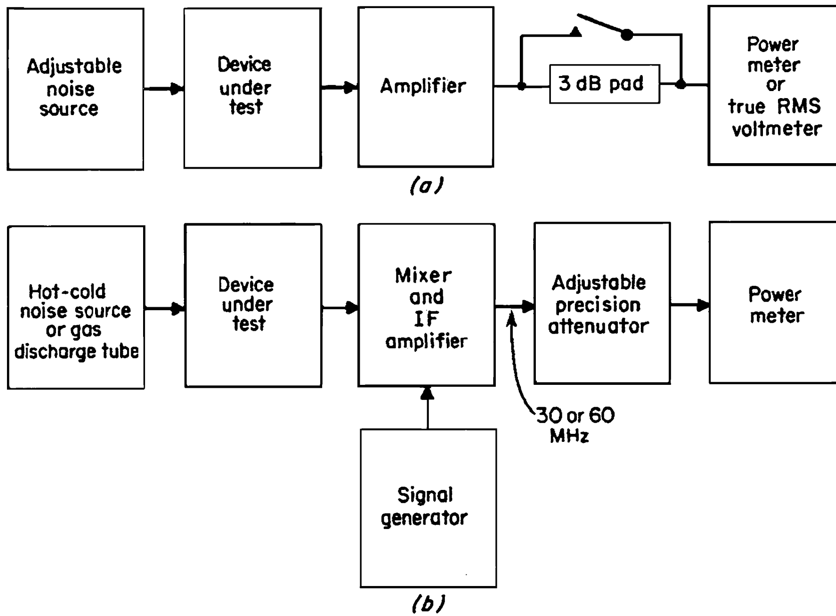

FIGURE 11.3.2 Noise-measurement techniques: (*a*) at low frequencies; (*b*) at high frequencies.

Several other techniques include the use of the H-P 8743 reflectometer, the general radio bridge GR 1607, the Rhode-Schwartz diagraph, and the H-P type 8510 microwave network analyzer to measure device parameters automatically from 45 MHz to 100 GHz with display and printout features.

Noise in RF Amplifiers

A common technique employing a noise source to measure the noise performance of an rf amplifier is shown in Fig. 11.3.2. Initially the external noise source (a temperature-limited diode) is turned off, the 3-dB pad short-circuited, and the reading on the output power meter recorded. The 3-dB pad is then inserted, the noise source is turned on, and its output increased until a reading equal to the previous one is obtained. The noise figure can then be read directly from the noise source, or calculated from 1 plus the added noise per unit bandwidth divided by the standard noise power available KT_0, where T_0 = 290 K and K = Boltzmann's constant = 1.38×10^{-23} J/K.

At higher frequencies, the use of a temperature-limited diode is not practical, and a gas-discharge tube or a hot-cold noise source is employed. The *Y*-factor technique of measurement is used. The output from the device to be measured is put into a mixer, and the noise output converted to a 30- or 60-MHz center-frequency (i.f.) output. A precision attenuator is then inserted between this i.f. output and the power-measuring device. The attenuator is adjusted to give the same power reading for two different conditions of noise power output represented by effective temperatures T_1 and T_2. The *Y* factor is the difference in decibels between the two precision attenuator values needed to maintain the same power-meter reading. The noise factor is

$$F = \frac{(T_2/290) - T_1 Y/290}{Y - 1} + 1$$

where T_1 = effective temperature at reference condition 1
T_2 = effective temperature of reference condition 2
Y = decibel reading defined in the text, converted to a numerical ratio

Downloaded from Digital Engineering Library @ McGraw-Hill (www.digitalengineeringlibrary.com)
Copyright © 2004 The McGraw-Hill Companies. All rights reserved.
Any use is subject to the Terms of Use as given at the website.

In applying this technique it is often necessary to correct for the second-stage noise. This is done by use of the cascade formula

$$F_1 = F_T - (F_2 - 1)/G_1$$

where F_1 = noise factor of first stage
F_T = overall noise factor measured
F_2 = noise factor of second-stage mixer and i.f. amplifier
G_1 = available gain of first stage

Large-Signal Performance of RF Amplifiers

The large-signal performance of an rf amplifier can be specified in many ways. A common technique is to specify the input where the departure from a straight-line input-output characteristic is 1 dB. This point is commonly called the *1-dB compression point*. The greater the input before this compression point is reached, the better the large-signal performance.

Another method of rating an rf amplifier is in terms of its third-order intermodulation performance. Here two different frequencies, f_1 and f_2, of equal powers, p_1 and p_2, are inserted into the rf amplifier, and the third frequency, internally generated, $2f_1 - f_2$ or $2f_2 - f_1$, has its power p_{12} measured. All three frequencies must be in the amplifier passband. With the intermodulation power p_{12} referred to the output, the following equation can be written:

$$P_{12} = 2P_1 + P_2 + K_{12}$$

where P_{12} = intermodulation output power at $2f_1 - f_2$ or $2f_2 - f_1$
P_1 = output power at input frequency f_1
P_2 = output power at input frequency f_2, all in decibels referred to (0 dBm)
K_{12} = constant associated with the particular device

The value of K_{12} in the above formula can be used to rate the performance of various device choices. Higher orders of intermodulation products can also be used.

A third measure of large-signal performance commonly used is that of cross-modulation. In this instance, a carrier at f_D with no modulation is inserted into the amplifier. A receiver is then placed at the output and tuned to this unmodulated carrier. A second carrier at f_1 with amplitude-modulation index M_I is then added. The power of P_I of f_I is increased, and its modulation is partially transferred to f_D. The equation becomes

$$10 \log (M_K/M_I) = P_I + K$$

where M_K = cross-modulation index of originally unmodulated signal at f_D
M_I = modulation index of signal F_I
P_I = output power of signal at f_I, all in decibels referred to 1 mW (0 dBm)
K = cross-modulation constant

Maximum Input Power

In addition to the large-signal performance, the maximum power of voltage input into an rf amplifier is specified, with a requirement that device burnout must not occur at this input. There are two ways of specifying this input: by a stated pulse of energy or by a requirement to withstand a continuously applied large signal. It is also common to specify the time required to unblock the amplifier after removal of the large input. With the increased use of field effect transistors (FETs especially) having good noise performance, these overload characteristics have become a severe problem. In many cases, conventional or zener diodes, in a back-to-back configuration shunting the input, are used to reduce the amount of power the input of the active devices must dissipate.

RF Amplifiers in Receivers

RF amplifiers intended for the first stages of receivers have additional restrictions placed on them. In most cases, such amplifiers are tunable across a band of frequencies with one or more tuned circuits. The tuned

Downloaded from Digital Engineering Library @ McGraw-Hill (www.digitalengineeringlibrary.com)
Copyright © 2004 The McGraw-Hill Companies. All rights reserved.
Any use is subject to the Terms of Use as given at the website.

RADIO-FREQUENCY AMPLIFIERS AND OSCILLATORS

circuits must track across the frequency band, and in the case of the superheterodyne, tracking of the local oscillator is necessary so that a constant frequency difference (i.f.) is maintained. The receiver's rf section can be tracked with the local oscillator by the two- or the three-point method, i.e., with zero error in the tracking at either two or three points.

A second consideration peculiar to rf amplifiers used for receivers is the AGC. This requirement is often stated by specifying a low-level rf input to the receiver and noting the power out. The rf signal input is then increased with the AGC applied until the output power has increased a predetermined amount. This becomes a measure of the AGC effectiveness. The AGC performance can also be measured by plotting a curve of rf input versus AGC voltage needed to maintain constant output, compared with the desired performance.

A third consideration in superheterodynes is the leakage of the local oscillator in the receiver to the outside. This spurious radiation is specified by the Federal Communications Commission (FCC) in the United States.

Design Using Immittance and Hybrid Parameters

The general gain and input-output impedance of an amplifier can be formulated, in terms of the Z or Y parameters, to be

$$Y_{\text{in}} = y_{11} - \frac{y_{12}y_{21}}{y_{22} + y_L} \qquad Y_{\text{out}} = y_{22} - \frac{y_{12}y_{21}}{y_{11} + y_s}$$

where y_L = load admittance
y_s = source admittance
Y_{in} = input admittance
Y_{out} = output admittance
G_T = transducer gain

and the transducer gain is

$$G_T = \frac{4\,\text{Re}\,y_s\,\text{Re}\,y_L\,|y_{21}|^2}{|(y_{11} + y_s)(y_{22} + y_L) - y_{12}y_{21}|^2}$$

for the y parameters, and interchange of z or y is allowed.

The stability of the circuit can be determined by either Linvill's C or Stern's k factor as defined below. Using the y parameters, $y_{ij} = g_{ik} + jB_{ik}$, these are

Linvill:
$$C = \frac{|y_{12}y_{21}|}{2g_{11}g_{22} - \text{Re}\,y_{12}y_{21}}$$

where $C < 1$ for stability does not include effects of load and source admittance.

Stern:
$$k = \frac{2(g_{11} + g_s)(g_{22} + g_L)}{|y_{12}y_{21}| + \text{Re}\,y_{12}y_{21}}$$

where $k > 1$ for stability
g_L = load conductance
g_s = source conductance

The preceding C factor defines only unconditional stability; i.e., no combination of load and source impedance will give instability. There is an invariant quantity K defined as

$$K = \frac{2\,\text{Re}\,\gamma_{11}\,\text{Re}\,\gamma_{22} - \text{Re}\,\gamma_{12}\gamma_{21}}{|\gamma_{21}\gamma_{12}|} \qquad \text{Re}\,\gamma_{11} > 0 \quad \text{Re}\,\gamma_{22} > 0$$

Downloaded from Digital Engineering Library @ McGraw-Hill (www.digitalengineeringlibrary.com)
Copyright © 2004 The McGraw-Hill Companies. All rights reserved.
Any use is subject to the Terms of Use as given at the website.

where γ represents either the y, z, g, or h parameters, and $K > 1$ denotes stability.

This quantity K has then been used to define maximum available power gain G_{max} (only if $K > 1$)

$$G_{max} = |\gamma_{21}/\gamma_{12}|(K - \sqrt{K^2 - 1})$$

To obtain this gain, the source and load immittance are found to be ($K > 1$)

$$\gamma_s = \frac{\gamma_{12}\gamma_{21} + |\gamma_{12}\gamma_{21}|(K + \sqrt{K^2 - 1})}{2\ \mathrm{Re}\,\gamma_{22}} - \gamma_{11} \qquad \gamma_s = \text{source immittance}$$

$$\gamma_L = \frac{\gamma_{12}\gamma_{21} + |\gamma_{12}\gamma_{21}|(K + \sqrt{K^2 - 1})}{2\ \mathrm{Re}\,\gamma_{11}} - \gamma_{22} \qquad \gamma_L = \text{load immittance}$$

The procedure is to calculate the K factor, and if $K > 1$, calculate G_{max}, γ_s, and γ_L. If $K < 1$, the circuit can be modified either by use of feedback or by adding immittances to the input-output.

Design Using *S* Parameters

The advent of automatic test equipment and the extension of vacuum tubes and transistors to be gigahertz frequency range have led to design procedures using the S parameters. Following the previous discussion, the input and output reflection coefficient can be defined as

$$p_{in} = S_{11} + p_L \frac{S_{12}S_{21}}{1 - p_L S_{22}} \qquad p_L = \frac{Z_L - Z_0}{Z_L + Z_0}$$

$$p_{out} = S_{22} + p \frac{S_{12}S_{21}}{1 - pS_{11}} \qquad p_s = \frac{Z_s - Z_0}{Z_s + Z_0}$$

where Z_0 = characteristic impedance
p_{in} = input reflection coefficient
p_{out} = output reflection coefficient

The transducer gain can be written

$$G_{transducer} = \frac{|S_{21}|^2 (1 - |p_s|^2)(1 - |p_L|^2)}{|(1 - S_{11}p_s)(1 - S_{22}p_L) - S_{21}S_{12}p_s p_L|^2}$$

The unconditional stability of the amplifier can be defined by requiring the input (output) impedance to have a positive real part for any load (source) impedance having a positive real part.

This requirement gives the following criterion:

$$|S_{11}|^2 + |S_{12}S_{21}| < 1 \qquad |S_{22}|^2 + |S_{12}/S_{11}| < 1$$

and

$$\eta = \frac{1 - |\Delta|^2 - |S_{11}|^2 - |S_{22}|^2}{2|S_{12}S_{21}|} > 1 \qquad \Delta_s = S_{11}S_{22} - S_{12}S_{21}$$

Downloaded from Digital Engineering Library @ McGraw-Hill (www.digitalengineeringlibrary.com)
Copyright © 2004 The McGraw-Hill Companies. All rights reserved.
Any use is subject to the Terms of Use as given at the website.

RADIO-FREQUENCY AMPLIFIERS AND OSCILLATORS

Similarly, the maximum transducer gain, for $\eta > 1$, becomes

$$G_{\text{max transducer}} = |S_{21}/S_{12}|(\eta \pm \sqrt{\eta^2 - 1})$$

(positive sign when $|S_{22}|^2 - |S_{11}|^2 - 1 + |\Delta_s|^2 > 0$) for conditions listed above.

The source and load to provide conjugate match to the amplifier when $\eta > 1$ are the solutions of the following equations, which give $|p_s|$, and $|p_L|$ less than 1

$$p_{ms} = C_1^* \frac{B_1 \pm \sqrt{B_1^2 - 4|C_1|^2}}{2|C_1|^2} \qquad p_{mL} = C_2^* \frac{B_2 \pm \sqrt{B_2^2 - 4|C_2|^2}}{2|C_2|^2}$$

where

$$B_1 = 1 + |S_{11}|^2 - |S_{22}|^2 - |\Delta_s|^2 \qquad B_2 = 1 + |S_{22}|^2 - |S_{11}|^2 - |\Delta_s|^2$$
$$C_1 = S_{11} - \Delta_s S_{22}^* \qquad C_2 = S_{22} - \Delta_s S_{11}^*$$

the star (*) denoting conjugate.

If $|\eta| > 1$ but η is negative or $|\eta| < 1$, it is not possible to match simultaneously the two-port with real source and load admittance. Both graphical techniques and computer programs are available to aid in the design of rf amplifiers.

Intermediate-Frequency Amplifiers

Intermediate-frequency amplifiers consist of a cascade of a number of stages whose frequency response is determined either by a filter or by tuned interstages. The design of the individual active stages follows the techniques discussed earlier, but the interstages become important for frequency shaping. There are various forms of interstage networks; several important cases are discussed below.

Synchronous-Tuned Interstages. The simplest forms of tuned interstages are synchronously tuned circuits. The two common types are the single- and double-tuned interstage.

The governing equations are:

1. Single-tuned interstage (Fig. 11.3.3*a*):

$$A(j\omega) = -A_r \frac{1}{1 + jQ_L(\omega/\omega_0 - \omega_0/\omega)}$$

where Q_L = loaded Q of the tuned circuit greater than 10
ω_0 = resonance frequency of the tuned circuit = $1\ \sqrt{LC}$
ω = frequency variable
A_r = midband gain equal to g_m times the midband impedance level

For an n-stage amplifier with n interstages,

$$A_T = A^n(j\omega) = A_r^n \left[1 + \left(\frac{\omega^2 - \omega_0^2}{B\omega}\right)^2\right]^{-n/2}$$

Downloaded from Digital Engineering Library @ McGraw-Hill (www.digitalengineeringlibrary.com)
Copyright © 2004 The McGraw-Hill Companies. All rights reserved.
Any use is subject to the Terms of Use as given at the website.

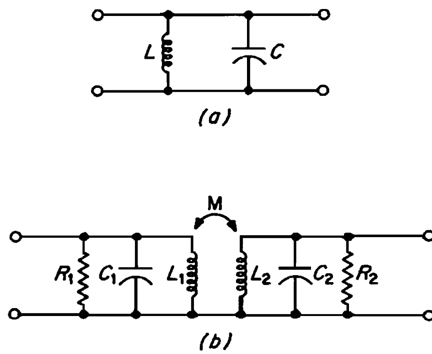

FIGURE 11.3.3 Interstage coupling circuits: (*a*) single-tuned; (*b*) double-tuned.

where $B = \omega_0/Q_L$ = single-stage bandwidth
n = number of stages
ω_0 = center frequencies
Q_L = loaded Q
$B_n = B\sqrt{2^{1/n}-1}$ is the overall bandwidth reduction owing to n cascades

2. Double-tuned interstage (Fig. 11.3.3*b*):

$$A(j\omega) = \frac{g_m k}{C_1C_2(1-k^2)\sqrt{L_1L_2}} \frac{j\omega}{\omega^4 - ja_1\omega^3 - a_2\omega^2 + ja_3\omega + a_4}$$

(for a single double-tuned stage), where

$$a_1 = \omega_r\left(\frac{1}{Q_1}+\frac{1}{Q_2}\right) \qquad a_2 = \frac{\omega_r^2}{Q_1Q_2} + \frac{1}{1-k^2}\left(\omega_1^2+\omega_2^2\right)$$

$$a_3 = \frac{\omega_r}{1+k^2}\left(\frac{\omega_2^2}{Q_1}+\frac{\omega_1^2}{Q_2}\right) \qquad a_4 = \frac{\omega_1^2\omega_2^2}{1-k^2}$$

The circuit parameters are

R_1 = total resistance primary side
C_1 = total capacitance primary side
L_1 = total inductance primary side
R_2 = total resistance secondary side
C_2 = total capacitance secondary side
L_2 = total inductance secondary side
M = mutual inductance = $k\sqrt{L_1L_2}$
k = coefficient of coupling

ω_r = resonant frequency of amplifier
$\omega_1 = 1/\sqrt{L_1C_1}$
$\omega_1 = 1/\sqrt{L_2C_2}$
Q_1 = primary Q at $\omega_r = \omega_r C_1 R_1$
Q_2 = secondary Q at $\omega_r = \omega_r C_2 R_2$
g_m = transconductance of active device at midband frequency

Simplification. If $\omega_1 = \omega_2 = \omega_0$, that is, primary and secondary tuned to the same frequency, then

$$\omega_r = \omega_0/\sqrt{1-k^2}$$

is the resonant frequency of the amplifier and

$$A(j\omega_r) = \frac{+jkg_m\sqrt{R_1R_2}}{\sqrt{Q_1Q_2}\,(k^2+1/Q_1Q_2)}$$

is the gain at this resonant frequency.

For maximum gain,

$$k_c = \frac{1}{\sqrt{Q_1Q_2}} = \text{critical coupling}$$

and for maximum flatness,

Downloaded from Digital Engineering Library @ McGraw-Hill (www.digitalengineeringlibrary.com)
Copyright © 2004 The McGraw-Hill Companies. All rights reserved.
Any use is subject to the Terms of Use as given at the website.

RADIO-FREQUENCY AMPLIFIERS AND OSCILLATORS

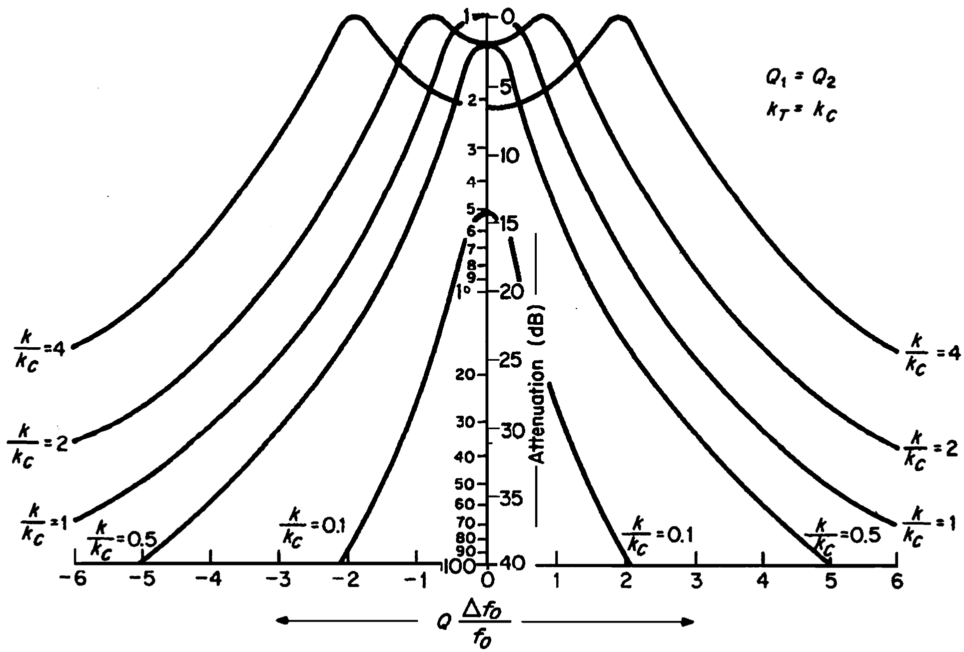

FIGURE 11.3.4 Selective curves for two identical circuits in a double-tuned interstage circuit, at various values of k/k_c.

$$k_T = \sqrt{\frac{1}{2}\left(\frac{1}{Q_1^2} + \frac{1}{Q_2^2}\right)} = \text{transitional coupling}$$

If k is increased beyond k_T, a double-humped response is obtained.

Overall bandwidth of an n-stage amplifier having equal Q circuits with transitional coupled interstages whose bandwidth is B is

$$B_n = B(2^{1/n} - 1)^{1/4}$$

The governing equations for the double-tuned-interstage case are shown above. The response for various degrees of coupling related to $k_T = k_C$ in the equal-coil-Q case is shown in Fig. 11.3.4.

Maximally Flat Staggered Interstage Coupling

This type of coupling consists of n single-tuned interstages that are cascaded and adjusted so that the overall gain function is maximally flat. The overall cascade bandwidth is B_n, the center frequency of the cascade is ω_c, and each stage is a single-tuned circuit whose bandwidth B and center frequency are determined from Table 11.3.1. The gain of each stage at cascade center frequency is $A(j\omega_c) = -g_m/C_T[B + j(\omega_c^2 - \omega_0^2/\omega_c]$, where C_T = sum of output capacitance and input capacitance to next stage and wiring capacitance of cascade, B = stage bandwidth, ω_0 = center frequency of stage, and ω_c = center frequency of cascade.

Downloaded from Digital Engineering Library @ McGraw-Hill (www.digitalengineeringlibrary.com)
Copyright © 2004 The McGraw-Hill Companies. All rights reserved.
Any use is subject to the Terms of Use as given at the website.

RADIO-FREQUENCY AMPLIFIERS AND OSCILLATORS

TABLE 11.3.1 Design Data for Maximally Flat Staggered *n*-tuples

n	Name of circuit	No. of stages	Center frequency of stage	Stage bandwidth
2	Staggered pair	2	$\omega_c \pm 0.35B_n$	$0.71B_n$
3	Staggered triple	2	$\omega_c \pm 0.43B_n$	$0.50B_n$
		1	ω_c	$1.00B_n$
4	Staggered quadruple	2	$\omega_c \pm 0.46B_n$	$0.38B_n$
		2	$\omega_c \pm 0.19B_n$	$0.92B_n$
5	Staggered quintuple	2	$\omega_c \pm 0.29B_n$	$0.81B_n$
		2	$\omega_c \pm 0.48B_n$	$0.26B_n$
		1	ω_c	$1.00B_n$
6	Staggered sextuple	2	$\omega_c \pm 0.48B_n$	$0.26B_n$
		2	$\omega_c \pm 0.35B_n$	$0.71B_n$
		2	$\omega_c \pm 0.13B_n$	$0.97B_n$
7	Staggered septuple	2	$\omega_c \pm 0.49B_n$	$0.22B_n$
		2	$\omega_c \pm 0.39B_n$	$0.62B_n$
		2	$\omega_c \pm 0.22B_n$	$0.90B_n$
		1	ω_c	$1.00B_n$

For $Q_L > 20$

RADIO-FREQUENCY OSCILLATORS

G. Burton Harrold

General Considerations

Oscillators at rf frequencies are usually of the class A sine-wave-output type.

RF oscillators (in common with audio oscillators) may be considered either as one-port networks that exhibit a negative real component at the input or as two-port-type networks consisting of an amplifier and a frequency-sensitive passive network that couples back to the input port of the amplifier. It can be shown that the latter type of feedback oscillator also has a negative resistance at one port. This negative resistance is of a dynamic nature and is best defined as the ratio between the fundamental components of voltage and current.

The sensitivity of the oscillator's frequency is directly dependent on the effective Q of the frequency-determining element and the sensitivity of the amplifier to variations in temperature, voltage variation, and aging. For example, the effective Q of the frequency-determining element is important because the percentage change in frequency required to produce the compensating phase shift in a feedback oscillator is inversely proportional to the circuit Q, thus the larger the effective Q the greater the frequency stability. The load on an oscillator is also critical to the frequency stability since it affects the effective Q and in many cases the oscillator is followed by a buffer stage for isolation.

It is also desirable to provide some means of stabilizing the oscillator's operating point, either by a regulated supply, dc feedback for bias stabilization, or oscillator self-biasing schemes such as grid-leak bias. This stabilizes not only the frequency but also the output amplitude, by tending to compensate any drift in the active device's parameters. It is also necessary to eliminate the harmonics in the output since they give rise to cross-modulation products producing currents at the fundamental frequency that are not necessarily in phase with the dominant oscillating mode. The use of high-Q circuits and the control of the nonlinearity helps in controlling harmonic output.

Negative-Resistance Oscillators

The analysis of the negative-impedance oscillator is shown in Fig. 11.3.5. The frequency of oscillation at buildup is not completely determined by the LC circuit but has a component that is dependent upon the circuit resistance. At steady state, the frequency of oscillation is a function of $1 + R/R_{iv}$ or $1 + R_{ic}/R$, depending on the particular circuit where the ratios R/R_{ic}, R_{iv}/R are usually chosen to be small. While R is a fixed function of the

Downloaded from Digital Engineering Library @ McGraw-Hill (www.digitalengineeringlibrary.com)
Copyright © 2004 The McGraw-Hill Companies. All rights reserved.
Any use is subject to the Terms of Use as given at the website.

RADIO-FREQUENCY AMPLIFIERS AND OSCILLATORS

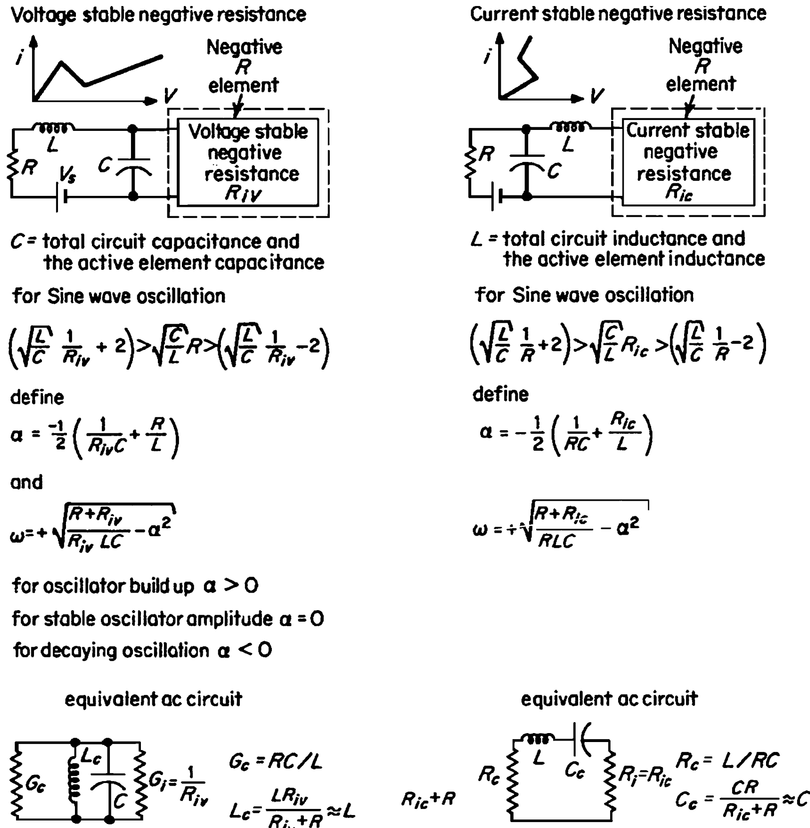

FIGURE 11.3.5 General analysis of negative-resistance oscillators.

loading, R_{ic} or R_{iv}/R must change with amplitude during oscillator buildup, so that the condition of $\alpha = 0$ can be reached. Thus R_{iv}, R_{ic} cannot be constant but are dynamic impedances defined as the ratio of the fundamental voltage across the elements to the fundamental current into the element.

The type of dc load for biasing and the resonant circuit required for the proper operation of a negative-resistance oscillator depend on the type of active element. R must be less than $|R_{iv}|$ or R must be greater than $|R_{ic}|$ in order for oscillation to build up and be sustained.

The detailed analysis of the steady-state oscillator amplitude and frequency can be undertaken by graphical techniques. The magnitude of G_i or R_i is expressed in terms of its voltage dependence. Care must be taken with this representation, since the shape of the G_i or R_i curve depends on the initial bias point.

The analysis of negative-resistance oscillators can now be performed by means of admittance diagrams. The assumption for oscillation to be sustaining is that the negative-resistance element, having admittance y_i, must equal $-y_c$, the external circuit admittance. This can be summarized by $G_i = -G_c$ and $B_i = -B_c$. A typical set of admittance curves is shown in Fig. 11.3.6. In this construction, it is assumed that $B_i = -B_c$, even during the oscillator buildup. Also shown is the fact that G_i at zero amplitude must be larger than G_c so that the oscillator can be started, that is, $\alpha > 0$, and that it may be possible to have two or more stable modes of oscillation.

Feedback Oscillators

Several techniques exist for the analysis of feedback oscillators. In the generalized treatment, the active element is represented by its y parameters whose element values are at the frequency of interest, having magnitudes

Downloaded from Digital Engineering Library @ McGraw-Hill (www.digitalengineeringlibrary.com)
Copyright © 2004 The McGraw-Hill Companies. All rights reserved.
Any use is subject to the Terms of Use as given at the website.

RADIO-FREQUENCY AMPLIFIERS AND OSCILLATORS

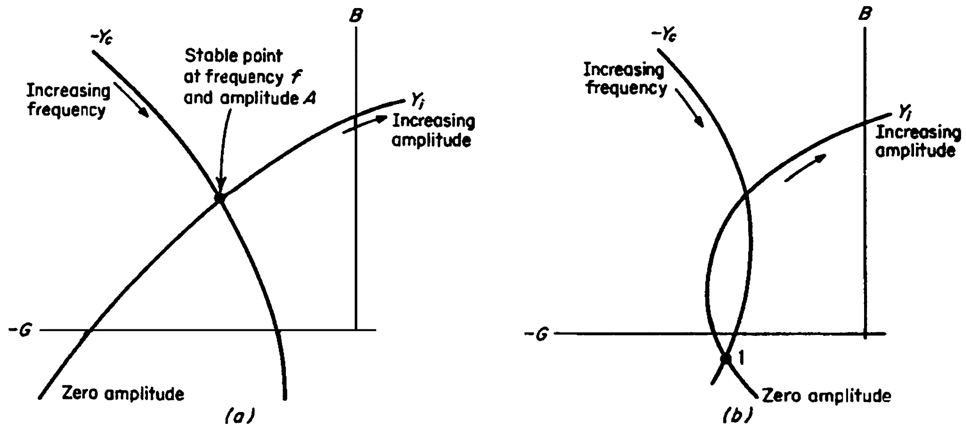

FIGURE 11.3.6 Admittance diagram of voltage-stable negative-resistance oscillators: (*a*) self-starting case, $\alpha > 0$; (*b*) circuit starts oscillating only if externally excited beyond point 1.

defined by the ratio of the fundamental current divided by fundamental voltage. The general block diagram and equations are shown in Fig. 11.3.7. Solution of the equations given yields information on the oscillator's performance. In particular, equating the real and imaginary parts of the characteristic equation gives information on amplitude and frequency of oscillation.

In many instances, many simplifications to these equations can be made. For example, if y_{11} and y_{12} are made small (as in vacuum-tube amplifiers), then

$$y_{21} = -(1/z_{21})(y_{22}z_{11} + 1) = -1/Z$$

This equation can be solved by equating the real and imaginary terms to zero to find the frequency and the criterion for oscillation of constant amplitude. This equation can also be used to draw an admittance diagram for oscillator analysis.

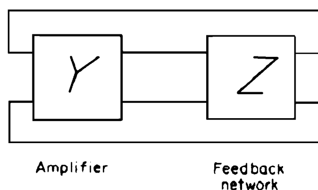

Amplifier

Feedback network

Characteristic equation:

$$y_{21}z_{21} + y_{11}z_{22} + y_{22}z_{11} + y_{12}z_{12} + \Delta_y\Delta_z + 1 = 0$$

$$\Delta_y = y_{11}y_{22} - y_{12}y_{21} \qquad \Delta_z = z_{11}z_{22} - z_{12}z_{21}$$

If $y_{21} >> y_{12}$ $\quad y_{12} \approx 0$ $\quad$ and $[z]$ passive $z_{12} = z_{21}$

Then:

$$y_{21}z_{12} + y_{11}z_{22} + y_{22}z_{11} + \Delta_y\Delta_z + 1 = 0$$

FIGURE 11.3.7 General analysis of feedback oscillators.

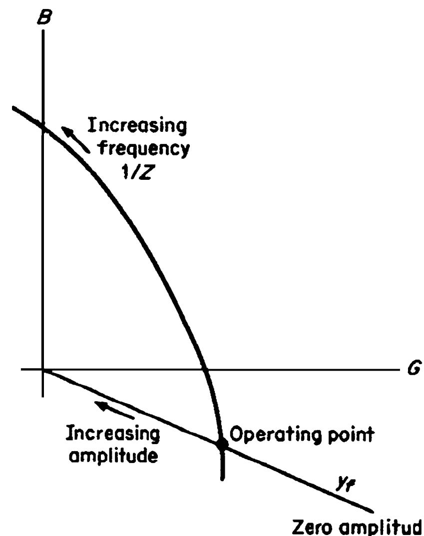

FIGURE 11.3.8 Admittance diagram of feedback oscillator.

Downloaded from Digital Engineering Library @ McGraw-Hill (www.digitalengineeringlibrary.com)
Copyright © 2004 The McGraw-Hill Companies. All rights reserved.
Any use is subject to the Terms of Use as given at the website.

RADIO-FREQUENCY AMPLIFIERS AND OSCILLATORS

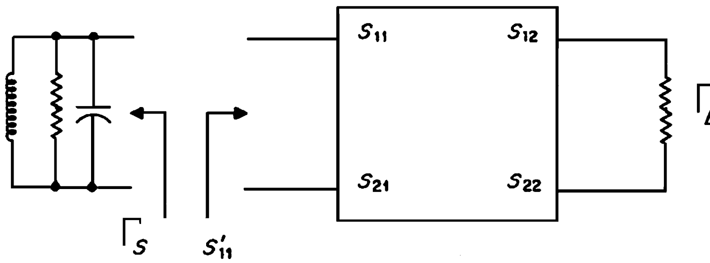

FIGURE 11.3.9 *S*-parameter and analysis of oscillators.

These admittance diagrams are similar to those discussed under negative-resistance oscillators. The technique is illustrated in Fig. 11.3.8.

At higher frequencies, the *S* parameters can also be used to design oscillators (Fig. 11.3.9). The basis for the oscillator is that the magnitude of the input reflection coefficient must be greater than unity, causing the circuit to be potentially unstable (in other words, it has a negative real part for the input impedance). The input reflection coefficient with a Γ_L output termination is

$$S'_{11} = S_{11} + \frac{S_{12}S_{21}\Gamma_L}{1 - S_{22}\Gamma_L}$$

Either by additional feedback or adjustment of Γ_L it is possible to make $|S'_{11}| > 1$. Next, establishing a load Γ_s such that it reflects all the energy incident on it will cause the circuit to oscillate. This criterion is stated as

$$\Gamma_L S'_{11} = 1$$

at the frequency of oscillation.

This technique can be applied graphically, using a Smith chart as before. Here the reciprocal of S'_{11} is plotted as a function of frequency since $S'_{11} > 1$. Now choose either a parallel or a series-tuned circuit and plot its Γ_s. If f_1 is the frequency common to $1/S'_{11}$ and Γ_s, and satisfies the above criterion, the circuit will oscillate at this point.

BROADBAND AMPLIFIERS

John W. Lunden, Jennifer E. Doyle

Introduction

In broadband amplifiers signals are amplified so as to preserve over a wide band of frequencies such characteristics as signal amplitude, gain response, phase shift, delay, distortion, and efficiency. The width of the band depends on the active device used, the frequency range, and power level in the current state of the art. As a general rule, above 100 MHz, a 20 percent or greater bandwidth is considered broadband, whereas an octave or more is typical below 100 MHz. As the state-of-the-art advances, it is becoming more common to achieve octave-bandwidth or wider amplifiers well into the microwave region using bipolar and FET active devices.

Hybrid-integrated-circuit techniques and new monolithic techniques eliminate many undesired package and bonding parasitics which can limit broadband amplifier performance. Additionally, distributed amplifiers, and other approaches which use multiple devices, have become more economical with increasing levels of integration.

It has become uncommon to use tube devices for new amplifier designs. Solid-state devices have replaced tubes in most amplifier applications because of superior long-term reliability and lower noise figures. In the following discussion both field-effect and bipolar transistor notations appear for generality.

Downloaded from Digital Engineering Library @ McGraw-Hill (www.digitalengineeringlibrary.com)
Copyright © 2004 The McGraw-Hill Companies. All rights reserved.
Any use is subject to the Terms of Use as given at the website.

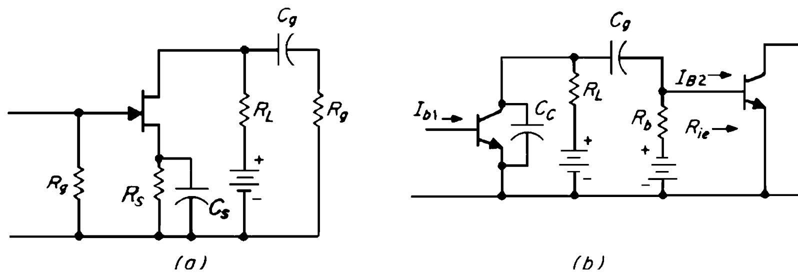

FIGURE 11.3.10 *RC*-coupled stages: (*a*) field-effect transistor form; (*b*) bipolar junction transistor form.

Low-, Mid-, and High-Frequency Performance

Consider the basic common-source and common-emitter-broadband *RC* coupled configurations shown in Fig. 11.3.10. Simplified low-frequency small-signal equivalent circuits are shown in Fig. 11.3.11.

The voltage gain of the FET amplifier stage under the condition that all reactances are negligibly small is the midband value (at frequency f)

$$(A_{\text{mid}})_{\text{FET}} = \frac{-g_m}{1/r_{ds} + 1/R_L + 1/R_g} \approx -g_m R_L$$

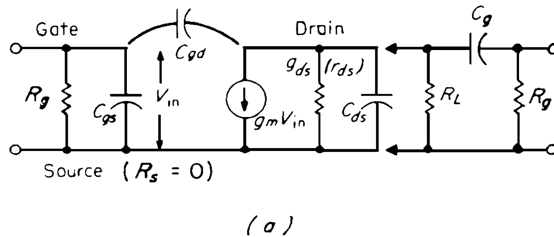

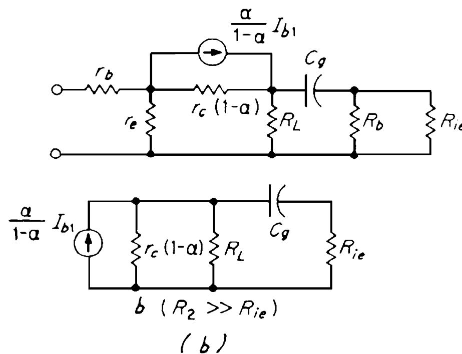

FIGURE 11.3.11 Equivalent circuits of the stages shown in Fig. 11.3.10: (*a*) FET form; (*b*) bipolar form.

Downloaded from Digital Engineering Library @ McGraw-Hill (www.digitalengineeringlibrary.com)
Copyright © 2004 The McGraw-Hill Companies. All rights reserved.
Any use is subject to the Terms of Use as given at the website.

RADIO-FREQUENCY AMPLIFIERS AND OSCILLATORS

If the low-frequency effects are included, this becomes

$$(A_{\text{low}})_{\text{FET}} = \frac{-g_m R_L}{1+1/j\omega R_g C_g} \frac{1+1/j\omega R_S C_S}{1+(1+g_m R_S)/j\omega C_S R_S} \left(= \frac{-g_m R_L}{1+1/j\omega R_g C_g} \text{for } R_S = 0 \right)$$

The low-frequency cutoff is because principally of two basic time constants, $R_g C_g$ and $R_S C_S$. For C_S values large enough for the time constant to be much longer than that associated with C_g, a low-frequency cutoff or half-power point can be determined as

$$(f_1)_{\text{FET}} = \frac{1}{2\pi C_g [R_g + r_{ds} R_L/(r_{ds} + R_L)]}$$

If the coupling capacitor is very large, the low-frequency cutoff is a result of C_S. The slope of the actual rolloff is a function of the relative effect of these two time constants. Therefore, the design of coupling and bypass circuits to achieve very-low-frequency response requires very large values of capacitance.

Similarly, for a bipolar transistor stage, the midband current gain can be determined as

$$(A_{\text{mid}})_{\text{BJT}} = \frac{-\alpha r_c R_L}{[R_L + r_c(1-\alpha)] \left[R_{ie} + \frac{R_L r_c (1-\alpha)}{R_L + r_c(1-\alpha)} \right]} \approx \frac{-\alpha}{1-\alpha} \frac{R_L}{R_L + R_{ie}}$$

where $$R_{ie} = r_b + \frac{r_e}{1-\alpha}$$

When low-frequency effects are included, this becomes

$$(A_{\text{low}})_{\text{BJT}} \approx \frac{-\alpha}{1-\alpha} \frac{R_L}{R_L + R_{ie} - j/\omega C_g} \quad \text{for } R_L \ll r_c(1-\alpha)$$

and

$$(f_1)_{\text{BJT}} = \frac{1}{2\pi C_g} \frac{1}{R_{ie} + \frac{R_L r_c (1-\alpha)}{R_L + r_c(1-\alpha)}} \approx \frac{1}{2\pi C_g} \frac{1}{R_{ie} + R_L}$$

If the ratio of low- to midfrequency voltage or current gain is taken, its reactive term goes to unity at $f = f_1$, that is, the cutoff frequency.

$$\frac{A_{\text{low}}}{A_{\text{mid}}} = \frac{1}{1 - j(f_1/f)} \qquad \phi_{\text{low}} = \tan^{-1} \frac{f_1}{f}$$

These quantities are plotted in Fig. 11.3.12 for a single time-constant rolloff.

Caution should be exercised in assuming that reactances between input and output terminals are negligible. Although this is generally the case, gain multiplicative effects can result in input or output reactance values greater than the values assumed above, e.g., by the Miller effect:

$$C_{\text{in}} = C_{gs} + C_{gd}(1 + g_m R_L')$$

Downloaded from Digital Engineering Library @ McGraw-Hill (www.digitalengineeringlibrary.com)
Copyright © 2004 The McGraw-Hill Companies. All rights reserved.
Any use is subject to the Terms of Use as given at the website.

RADIO-FREQUENCY AMPLIFIERS AND OSCILLATORS

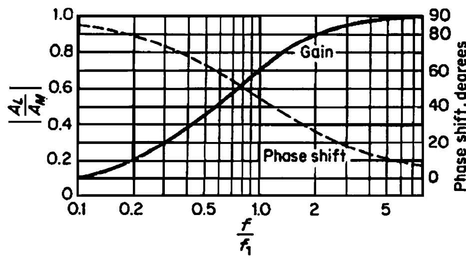

FIGURE 11.3.12 Gain and phase-shift curves at low frequencies.

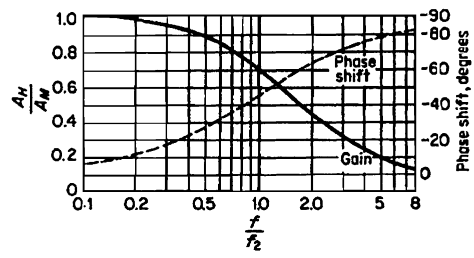

FIGURE 11.3.13 Gain and phase-shift curves at high frequencies.

Typically, the midfrequency gain equation can be used for frequencies above that at which $X_c = R_g/10$ below that at which $X_{cg} = 10R_gR_L/(R_g + R_L)$ (for the FET circuit).

If the frequency is increased further, a point is reached where the shunt reactances are no longer high with respect to the circuit resistances. At this point the coupling and bypass capacitors can be neglected. The high-frequency gain can be determined as

$$(A_{\text{high}})_{\text{FET}} = \frac{-g_m}{1/r_{ds} + 1/R_L + j\omega C_L}$$

where C_L is the effective total interstage shunt capacitance.

$$(A_{\text{high}})_{\text{BJT}} \approx \frac{-\alpha}{1-\alpha} \frac{1}{1 + R_{ie}\left(\dfrac{1}{R_L} + \dfrac{j\omega C_c}{1-\alpha}\right)} \quad \text{for } R_L \ll r_c(1-\alpha)$$

The ratio of high- to midfrequency gains can be taken and upper cutoff frequencies determined

$$\left(\frac{A_{\text{high}}}{A_{\text{mid}}}\right)_{\text{FET}} = \frac{1}{1 + j\omega C_L \dfrac{1}{(1/r_{ds}) + (1/R_L) + (1/R_g)}}$$

$$(f_2)_{\text{FET}} = \frac{1}{2\pi C_L}\left(\frac{1}{r_{ds}} + \frac{1}{R_L} + \frac{1}{R_g}\right)$$

$$\left(\frac{A_{\text{high}}}{A_{\text{mid}}}\right)_{\text{BJT}} = \frac{1}{1 + \dfrac{j\omega C_c r_c R_L R_{ie}}{R_{ie}[R_L + r_c(1-\alpha)] + R_L r_c(1-\alpha)}}$$

$$(f_2)_{\text{BJT}} \approx \frac{1-\alpha}{2\pi C_c}\left(\frac{1}{R_L} + \frac{1}{R_{ie}}\right) \quad \text{and} \quad \phi_{\text{high}} = -\tan^{-1}(f/f_2)$$

Dimensionless curves for these gain ratios and phase responses are plotted in Fig. 11.3.13.

Compensation Techniques

To extend the cutoff frequencies f_1 and f_2 to lower or higher values, respectively, compensation techniques can be used.

Downloaded from Digital Engineering Library @ McGraw-Hill (www.digitalengineeringlibrary.com)
Copyright © 2004 The McGraw-Hill Companies. All rights reserved.
Any use is subject to the Terms of Use as given at the website.

RADIO-FREQUENCY AMPLIFIERS AND OSCILLATORS

Figure 11.3.14 illustrates two techniques for low-frequency compensation. If the condition $R_gC_g = C_XR_XR_L/(R_X + R_L)$ is fulfilled (in circuit *a* or *b*), the gain relative to the midband gain is

$$\frac{A_{\text{low}}}{A_{\text{mid}}} = \frac{1}{1 - j(1/\omega R_g C_g)[R_L/(R_L + R_X)]} \quad \text{and} \quad f_1 = \frac{1}{2\pi R_g C_g}\frac{R_L}{R_L + R_X}$$

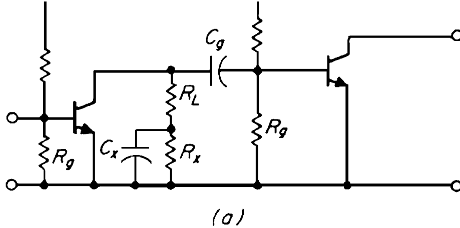

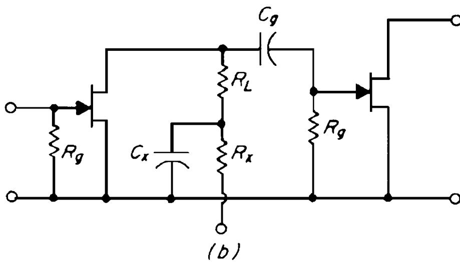

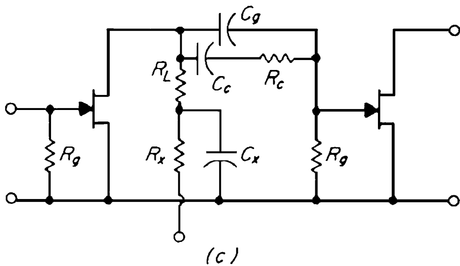

FIGURE 11.3.14 Low-frequency compensation networks: (*a*) bipolar transistor version; (*b*), (*c*) FET versions.

Hence, improved low-frequency response is obtained with increased values of R_X. This value is related to R_L and restricted by active-device operating considerations. Also, R_L is dependent on the desired high-frequency response. It can be shown that equality of time constants $R_LC_X = R_gC_g$ will produce zero phase shift in the coupling circuit (for $R_X > 1/\omega C_x$). The circuit shown in Fig. 11.3.14*c* is more critical. It is used with element ratios set to $R_L/R_X = R_g/R_c$ and $C_X/C_g = R_c/R_X$.

Various compensation circuits are also available for high-frequency-response extension. Two of the most common, the series- and shunt-compensation cases, are shown in Fig. 11.3.15. The high-frequency-gain expressions of these configurations can be written

$$\left|\frac{A_{\text{high}}}{A_{\text{mid}}}\right| = \sqrt{\frac{1 + a_1(f/f_2)^2 + a_2(f/f_2)^4 + \cdots}{1 + b_1(f/f_2)^2 + b_2(f/f_2)^4 + b_3(f/f_2)^6 + \cdots}}$$

The coefficients of the terms decrease rapidly for the higher-order terms, so that if $a_1 = b_1$, $a_2 = b_2$, etc., to as high an order of the f/f_2 ratio as possible, a maximally flat response curve is obtained.

For the phase response, $d\phi/d\omega$ can also be expressed as a ratio of two polynomials in f/f_2, and a similar procedure can be followed. A flat time-delay curve results. Unfortunately, the sets of conditions for flat gain and linear phase are different, and compromise values must be used.

Shunt Compensation. The high-frequency gain and time delay for the shunt-compensated stage are

$$\left|\frac{A_{\text{high}}}{A_{\text{mid}}}\right| = \sqrt{\frac{1 + \alpha^2(f/f_2)^2}{1 + (1 - 2\alpha)(f/f_2)^2 + \alpha^2(f/f_2)^4}} \qquad \phi = -\tan^{-1}\frac{f}{f_2}\left[1 - \alpha + \left(\frac{f}{f_2}\right)^2\alpha^2\right]$$

where $a = L/C_gR_L^2$ and $R_g \gg R_L$.

A case when R_g cannot be assumed to be high, such as the input of a following bipolar transistor stage, is considerably more complex, depending on the transistor equivalent circuit used. This is particularly true when operating near the transistor f_T and/or above the VHF band.

Series Compensation. In the series-compensated circuit, the ratio of C_s to C_g is an additional parameter. If this can be optimized, the circuit performance is better than in the shunt-compensated case. Typically, however, control of this parameter is not available due to physical and active-device constraints.

Downloaded from Digital Engineering Library @ McGraw-Hill (www.digitalengineeringlibrary.com)
Copyright © 2004 The McGraw-Hill Companies. All rights reserved.
Any use is subject to the Terms of Use as given at the website.

RADIO-FREQUENCY AMPLIFIERS AND OSCILLATORS

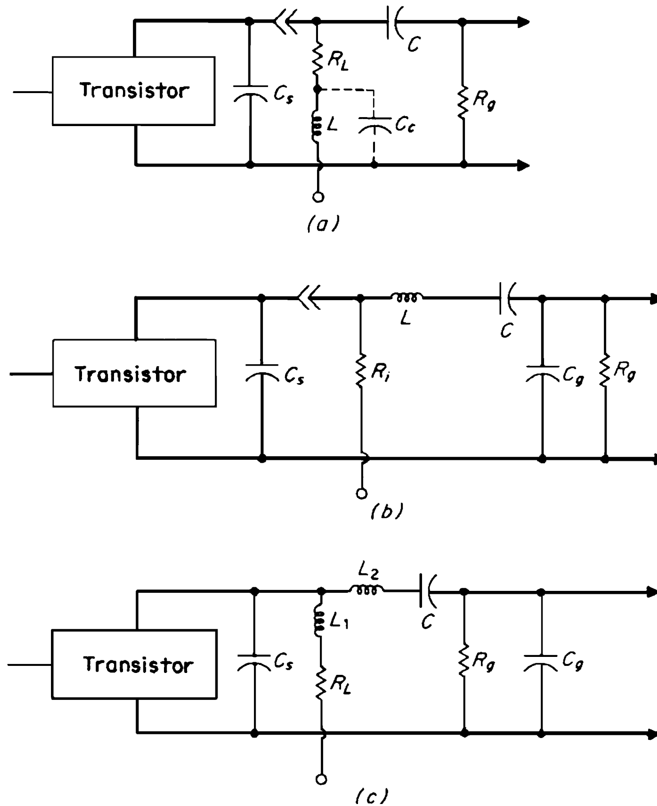

FIGURE 11.3.15 High-frequency compensation schemes: (*a*) shunt; (*b*) series; (*c*) shunt-series.

These two basic techniques can be combined to improve the response at the expense of complexity. The shunt-series-compensation case and the so-called "modified" case are examples. The latter involves a capacitance added in shunt with the inductance L or placing L between C_s and R_L.

For the modified-shunt case, the added capacitance C_c permits an additional degree of freedom, and associated parameter, $k_1 = C_c/C_s$.

Other circuit variations exist for specific broadband compensation requirements. Phase compensation, for example, may be necessary as a result of cascading a number of minimum-phase circuits designed for flat frequency response. Circuits such as the lattice and bridged-T can be used to alter the system response by reducing the overshoot without severely increasing the overall rise time.

Cascaded Broadband Stages

When an amplifier is made up of n cascaded RC stages, not necessarily identical, the overall gain A_n can be written

$$\left|\frac{A_n}{A_{\text{mid}}}\right| = \left[\frac{1}{1+(f/f_a)^2}\right]^{1/2}\left[\frac{1}{1+(f/f_b)^2}\right]^{1/2}\cdots\left|\frac{1}{1+(f/f_n)^2}\right|^{1/2}$$

Downloaded from Digital Engineering Library @ McGraw-Hill (www.digitalengineeringlibrary.com)
Copyright © 2004 The McGraw-Hill Companies. All rights reserved.
Any use is subject to the Terms of Use as given at the website.

RADIO-FREQUENCY AMPLIFIERS AND OSCILLATORS

where $f_a, f_b, \ldots, f_n$ are the f_1 or f_2 values for the respective stages, depending on whether the overall low- or high-frequency gain ratio is being determined. The phase angle is the sum of the individual phase angles. If the stages are identical, $f_a = f_b = f_x$ for all, and

$$\left|\frac{A_n}{A_{\text{mid}}}\right| = \left|\frac{1}{1+(f/f_x)^2}\right|^{n/2}$$

Stagger Peaking. In stagger tuning a number of individual bandpass amplifier stages are cascaded with frequencies skewed according to some predetermined criteria. The most straightforward is with the center frequencies adjusted so that the f_2 of one stage concludes with the f_1 of the succeeding stage, and so forth. The overall gain bandwidth then becomes

$$(\text{GBW})_n = \sum_{n=1}^{N} (\text{GBW})_n$$

A significant simplifying criterion of this technique is stage isolation. Isolation, in transistor stages particularly, is not generally high, except at low frequencies. Hence the overall design equations and subsequent overall alignment can be significantly complicated because of the interactions. Complex device models and computer-aided design greatly facilitate the implementation of this type of compensation. The simple shunt-compensated stage has found extensive use in stagger-tuned pulse-amplifier applications.

Transient Response

Time-domain analysis is particularly useful for broadband applications. Extensive theoretical studies have been made of the separate effects of nonlinearities of amplitude and phase response. These effects can be investigated starting with a normalized low-pass response function.

$$A(j\omega)/A(0) = \exp\,(a^m w^m - jb^n w^n)$$

where a and m are constants describing amplitude-frequency response and b and n are constants describing phase-frequency response. Figure 11.3.16 illustrates the time response to an impulse and a unit-step forcing function for various values of m, with $n = 0$. Rapid change of amplitude with frequency (large m) results in

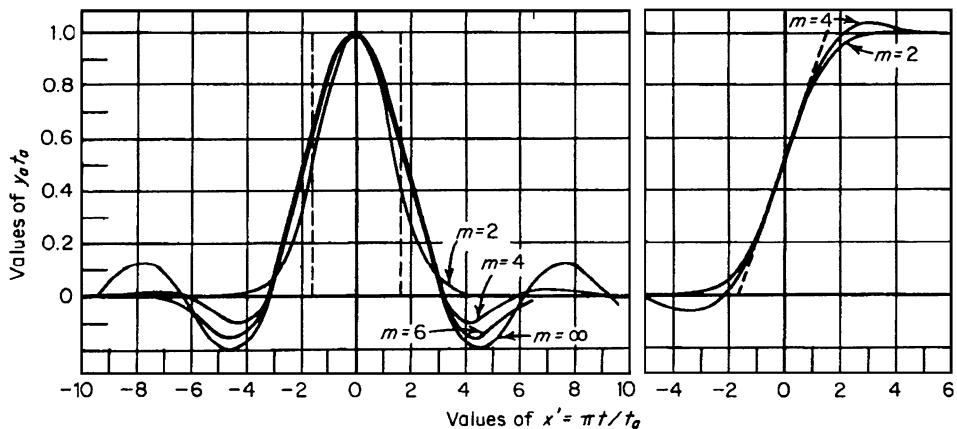

FIGURE 11.3.16 Transient responses to unit impulse (*left*) and unit step (*right*) for various values of m.

Downloaded from Digital Engineering Library @ McGraw-Hill (www.digitalengineeringlibrary.com)
Copyright © 2004 The McGraw-Hill Companies. All rights reserved.
Any use is subject to the Terms of Use as given at the website.

RADIO-FREQUENCY AMPLIFIERS AND OSCILLATORS

overshoot. Nonzero, but linear, phase-frequency characteristics ($n = 1$) result in a delay of these responses, without introducing distortion. Further increase in n results in increased ringing and asymmetry of the time function.

An empirical relationship between rise time (10 to 90 percent) and bandwidth (3 dB) can be expressed as

$$t_r \cdot \text{BW} = K$$

where K varies from about 0.35 for circuits with little or no overshoot to 0.45 for circuits with about 5 percent overshoot. K is 0.51 for the ideal rectangular low-pass response with 9 percent overshoot; for the Gaussian amplitude response with no overshoot, $K = 0.41$.

The effect on rise time of cascading a number of networks n depends on the individual network pole-zero configurations. Some general rules follow.

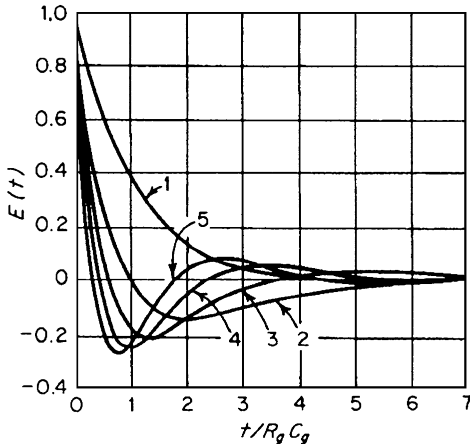

FIGURE 11.3.17 Response to a unit step of n capacitively coupled stages of the same time constant.

1. For individual circuits having little or no overshoot, the overall rise time is

$$t_{rt} = (t_{r1}^2 + t_{r2}^2 + t_{r3}^2 + \cdots)^{1/2}$$

2. If $t_{r1} = t_{r2} = t_{rn}$,

$$t_{rt} = 1.1\sqrt{nt_{r1}}$$

3. For individual stage overshoots of 5 to 10 percent, total overshoot increases as $\sqrt{n}$.
4. For circuits with low overshoot (~1 percent), the total overshoot is essentially that of one stage.

The effect of insufficient low-frequency response of an amplifier is sag of the time response. A small amount of sag (<10 percent) can be described by the formula

$$E_{\text{sag}}/E_{\text{tot}} = T/2.75RC$$

where T is one-half period of a square-wave voltage.

Figure 11.3.17 illustrates the response to a step function of n capacitor-coupled stages with the same time constant. The effect of arithmetic addition of individual stage initial slopes determining the net total initial transition slope can be seen.

Distributed Amplifiers

This technique is useful for operation of devices at or near the high-frequency limitation of gain bandwidth. While the individual stage gain is low, the stages are cascaded so that the gain response is additive instead of multiplicative. The basic principle is to allow the input and output capacitances to form the shunt elements of two delay lines. This is shown in Fig. 11.3.18.

If the delay times per section in the two lines are the same, the output signals traveling forward add together without relative delay. Care must be taken to ensure proper terminating conditions. The gain produced by n devices, each of transconductance g_m, has a value of $G = ng_mZ_{02}/2$. Performance to very low frequencies can be achieved. The high-frequency limit is determined by the cutoff frequencies of the input and output lines or effects within the active devices themselves other than parasitic shunt capacities (e.g., transit time or alpha-fall-off effects).

For input and output lines of different characteristic impedances, the overall gain is given by

$$G = \frac{2Z_{01}}{Z_{01} + Z_{02}} \frac{ng_mZ_{02}}{2}$$

Downloaded from Digital Engineering Library @ McGraw-Hill (www.digitalengineeringlibrary.com)
Copyright © 2004 The McGraw-Hill Companies. All rights reserved.
Any use is subject to the Terms of Use as given at the website.

RADIO-FREQUENCY AMPLIFIERS AND OSCILLATORS

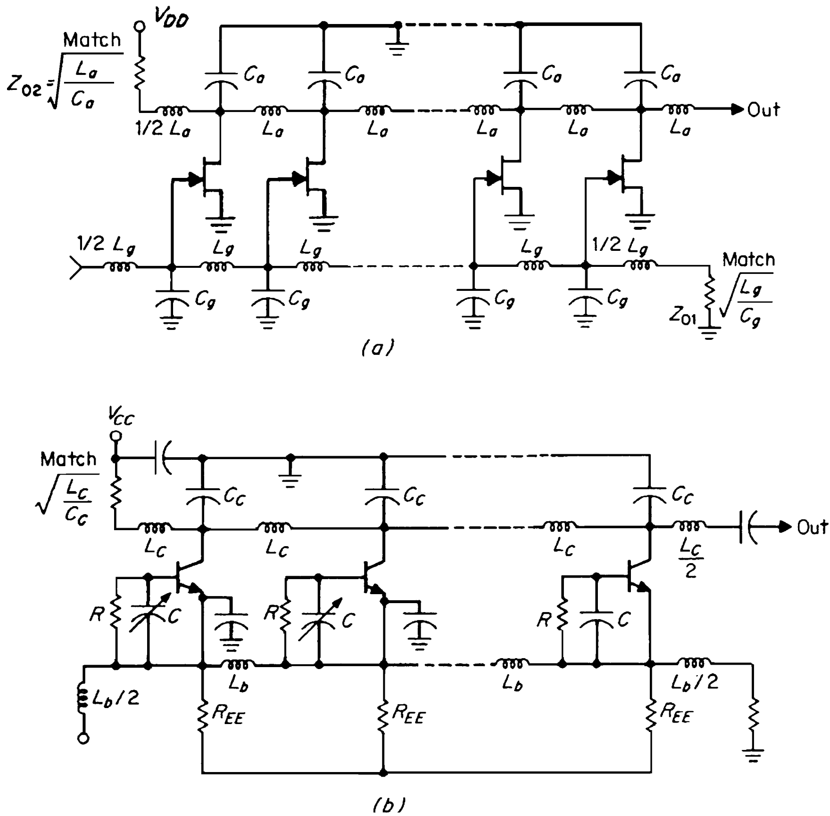

FIGURE 11.3.18 Distributed amplifier circuits: (*a*) FET version; (*b*) bipolar transistor version.

The characteristic impedances and cutoff frequencies are given as

$$Z_{01} = \sqrt{L_g/C_g} \qquad Z_{02} = \sqrt{L_a/C_a}$$
$$f_{c1} = \pi/\sqrt{L_g C_g} \qquad f_{c2} = \pi/\sqrt{L_a C_a}$$

There does not seem to be an optimum choice for Z_{02}; a device with a high figure of merit is simply chosen, and the rest follows. There is, however, an optimum way in which N devices can be grouped, namely, in m identical cascaded stages, each with n devices, so that N is a minimum for a given overall gain A. N is a minimum when $m = \ln A$. Consequently, the optimum gain per stage $G = e = 2.72$.

Various techniques are utilized to determine the characteristics of the lumped transmission lines. Constant-K and m-derived filter sections are most common, augmented by several compensation circuit variations. The latter include paired gate-drain (base-collector), bridged-T, and resistive loading connections. The constant-K lumped line has several limitations, including the fact that the termination is not a constant resistance and that impedance increases with frequency and time delay also changes with frequency.

m-derived terminating half sections and time-delay equalizing sections result in a frequency-amplitude response that is quite flat at very high frequencies.

The effects of input loading and/or line loss modify the gain expression to

$$G = \frac{2(GB)}{f_c}\,\frac{e^{-a}(1-e^{-n\propto})}{1-e^{-\propto}}$$

Downloaded from Digital Engineering Library @ McGraw-Hill (www.digitalengineeringlibrary.com)
Copyright © 2004 The McGraw-Hill Companies. All rights reserved.
Any use is subject to the Terms of Use as given at the website.

RADIO-FREQUENCY AMPLIFIERS AND OSCILLATORS

where $\propto$ = the real part of propagation constant γ and

$$GB = \frac{g_m}{2\pi C_{\text{eff}}}\bigg|_{\text{FET}}$$

The design of distributed amplifiers using bipolar transistors is more difficult because of the low input impedance. In addition, the intrinsic gain of the transistor (β or α) is a decreasing function of frequency.

The simplest approach in overcoming this problem is to connect a parallel RC in series with the base, as shown in Fig. 11.3.18*b*. By setting $RC = \beta_0/2\pi f_T$, the gain is made essentially independent of frequency up to about $f_T/2$, with an overall voltage gain of

$$A_\upsilon = (n\beta_0 Z_0/2R)^m$$

where m is the number of stages and n is the number of transistors per stage.

The increasing impedance of the constant-K line helps keep the frequency response flat, compensating for the increased loading of the bipolar transistor.

Another bipolar transistor approach involves the division of the frequency range into three regions to account for the losses. Each region is associated with a linear-Q variation with frequency of the transistor input-output circuits, approximated by shunt RC elements.

$$Q_{\text{in}} = w(C_{\text{in}} + C)/(G_{\text{in}} + G_k)$$

The lossless voltage gain is

$$A_L = f_T Z_0/\{2f\,[1 - (f/f_c)^2]^{1/2}\}$$

In region I, the input impedance is high and the transistor supplies high voltage gain. In regions II and III, the voltage gains are given by

$$A_{\text{II}} = A_L n \frac{1 - nK_{\text{II}} Z_0 (f/f_c)^2}{4r_b'[1-(f/f_c)^2]^{1/2}} \qquad A_{\text{III}} = A_L n \frac{1 - nK_{\text{III}} Z_0}{4r_b'[1-(f/f_c)^2]^{1/2}}$$

where $K_{\text{II}} = (f_c/f_Q)^2$

$K_{\text{III}} = 1$

f_Q = frequency of min Q

Broadband Matching Circuits

Broadband impedance transformation interstage-coupling matching can be achieved with balun transformers, quarter-wave transmission-line sections, lumped reactances in configurations other than discussed above, and short lengths of transmission lines.

Balun Transformers. In conventional coupling transformers, the interwinding capacitance resonates with the leakage inductance, producing a loss peak. This limits the high-frequency response. A solution is to use transmission-line transformers in which the turns are arranged physically to include the interwinding capacitance as a component of the characteristic impedance of a transmission line. With this technique, bandwidths of hundreds of megahertz can be achieved. Good coupling can be realized without resonances, leading to the use of these transformers in power dividers, couplers, hybrids, and so forth.

Typically, the lines take the form of twisted wire pairs, although coaxial lines can also be used. In some configurations, the length of the line determines the upper cutoff frequency. The low-frequency limit is determined by the primary inductance. The larger the core permeability the fewer the turns required for a given low-frequency response. Ferrite toroids have been found to be satisfactory with widely varying core-material

Downloaded from Digital Engineering Library @ McGraw-Hill (www.digitalengineeringlibrary.com)
Copyright © 2004 The McGraw-Hill Companies. All rights reserved.
Any use is subject to the Terms of Use as given at the website.

RADIO-FREQUENCY AMPLIFIERS AND OSCILLATORS

characteristics. The decreasing permeability with increasing frequency is offset by the increasing reactance of the wire itself, causing a wide-band, flat-frequency response.

Quarter-Wave Transformers. The quarter-wavelength line transformer is another well-known element. It is simply a transmission line one-quarter wavelength long, with a characteristic impedance

$$Z_{\text{line}} = \sqrt{Z_{\text{in}} Z_{\text{out}}}$$

where Z_{in} and Z_{out} are the terminating impedances. The insertion loss of this line section is

$$10 \log\left[1 + \frac{(r-1)^2}{4r} \cos^2\theta\right] \qquad \text{(dB)}$$

where $r = Z_{\text{in}}/Z_{\text{out}}$ and $\theta = 2\pi L/\lambda = 90°$ at f_0.

Figure 11.3.19 shows the bandwidth performance of the quarter-wave line for several matching ratios. Such lines may be cascaded to achieve broader-band matching by reducing the matching ratio required of each individual section.

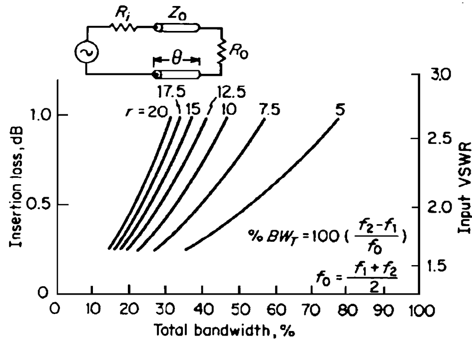

FIGURE 11.3.19 Bandwidth of a quarter-wave matching transformer.

Lumped and Pseudo-Lumped Transformations. The familiar lumped-element ladder network, depending on the element values and realization, approximates a short-step transmission-line transformer or a tapered transmission line.

Feedback and Gain Compensation

Feedback. The bandwidth of amplifiers can be increased by the application of inverse feedback. A multiplicity of feedback combinations and analysis techniques are available and extensively treated in the literature. In addition, the related concept of feedforward has been investigated and successfully implemented. Figure 11.3.20 shows four feedback arrangements and formulas describing their performance. A major consideration, particularly for rf applications, is the control of impedance and loop-delay characteristics to ensure stability.

Gain Compensation. The power gain of a bipolar transistor amplifier typically falls 6 dB/octave with increasing frequency above the f_β value. The gain can be leveled (bandwidth-widened) by exact matching of the source impedance to the device at the upper frequency only, causing increasing mismatch with decreasing frequency and the associated gain loss. The overall flat gain is the value at the high best-match frequency. Sufficient resistive loss is usually required in this interstage to prevent instabilities in either driver or driven stage because of the mismatch unloading.

Power-Combining Amplifiers

Many circuit techniques have been developed to obtain relatively high output powers with given modest-power devices. Two approaches are the direct-paralleling and hybrid splitting-combining techniques. The direct-paralleling approach is limited by device-to-device variations and the difficulties in providing balanced conditions because of the physical wavelength restrictions. A technique commonly used at UHF and microwave frequencies to obtain multioctave response incorporates matched stages driven from hybrid couplers in a balanced configuration. The coupler offers a constant-source impedance (equal to the driving-port

Downloaded from Digital Engineering Library @ McGraw-Hill (www.digitalengineeringlibrary.com)
Copyright © 2004 The McGraw-Hill Companies. All rights reserved.
Any use is subject to the Terms of Use as given at the website.

RADIO-FREQUENCY AMPLIFIERS AND OSCILLATORS

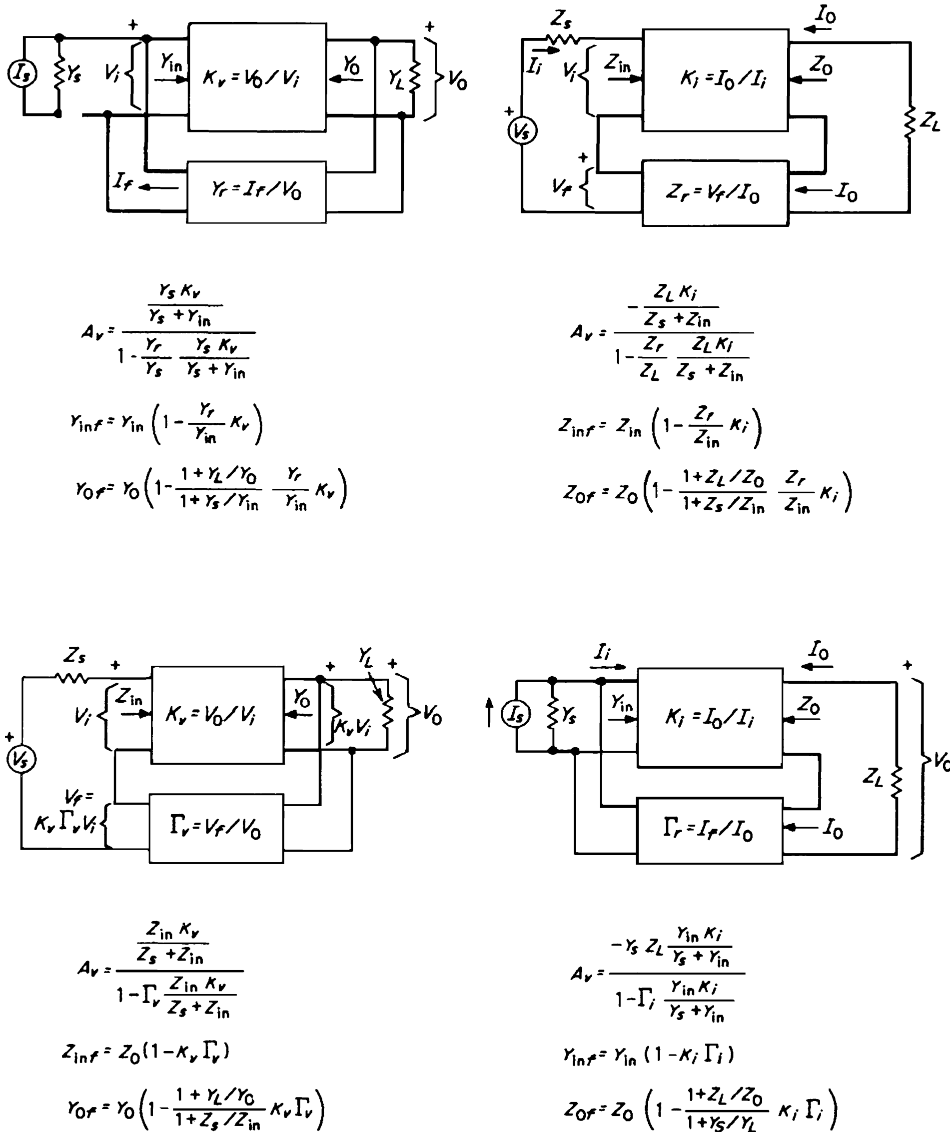

FIGURE 11.3.20 Four methods of applying feedback, showing influence on gain and input and output immittances (*From Hakim "Junction Transistor Circuit Analysis," by permission of John Wiley & Sons, New York*).

impedance) to the two stages connected to its output ports. Power reflected because of the identical mismatches is coupled to the difference port of the hybrid and dissipated in the idler load. The hybrid splitting-combining approach has proved quite effective in implementing high-output-level requirements (e.g., kilowatts at 1.4 GHz with bipolar transistors).

The hybrid splitting-combining approach enhances circuit operation. In particular, quadrature hybrids affect a voltage standing wave ratio (VSWR)-canceling phenomenon that results in extremely well-matched

Downloaded from Digital Engineering Library @ McGraw-Hill (www.digitalengineeringlibrary.com)
Copyright © 2004 The McGraw-Hill Companies. All rights reserved.
Any use is subject to the Terms of Use as given at the website.

RADIO-FREQUENCY AMPLIFIERS AND OSCILLATORS

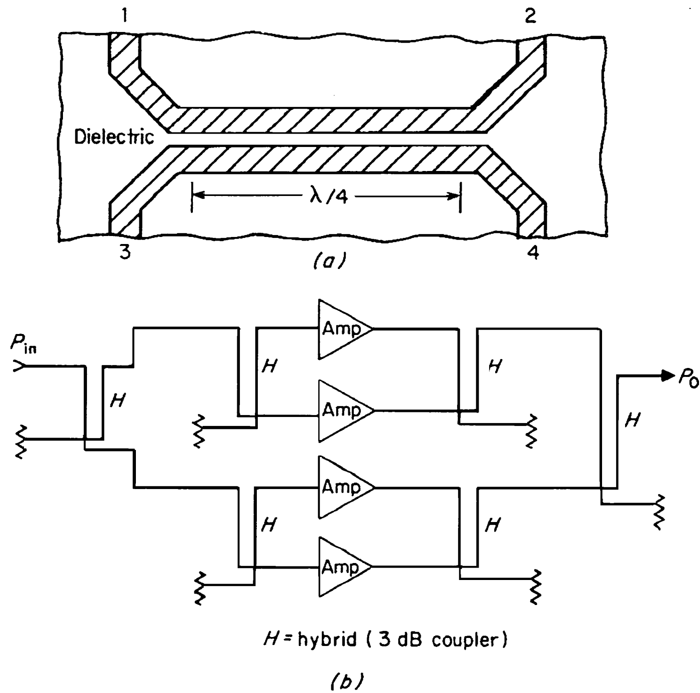

FIGURE 11.3.21 Wide-band combining techniques: (*a*) wide-band quarter-wave coupler; (*b*) balanced combining amplifier configuration.

power-amplifier inputs and outputs that can be broadbanded on proper selection of particular hybrid trees. Also, the excellent isolation between devices makes reliable power-amplifier service possible.

Several hybrid-directional-coupler configurations are possible, including the split-T, branch-line, magic-T, backward-wave, and lumped. Important factors in the choice of hybrid for this application are coupling bandwidth, isolation, fabrication ease, and form. The equiamplitude, quadrature-phase, reverse-coupled transverse electromagnetic wave (TEM) $\lambda/4$ coupler is a particularly attractive implementation owing to its bandwidth and amenability to strip-transmission-line circuits. Figure 11.3.21 illustrates this coupler type. Other commonly used broadband microstrip hybrids include the Wilkinson and the Lange couplers.

Integrated Amplifiers

As broadband amplifier designs are extended into microwave frequencies, package parasitics begin to limit high-frequency performance. A hybrid integrated circuit (HIC) has transmission paths and passive components formed together on a low-loss substrate by etching and deposition techniques. Active devices, and some discrete passive components, are then connected to the substrate transmission paths by beam-leading, soldering, or wire bonding. The active devices may be chips, packaged devices, or chips mounted on carriers. HICs show improved high-frequency performance because of minimal lead lengths, and transmission lines which provide impedance matching.

The monolithic microwave integrated circuit (MMIC) includes all active devices, as well as passive components and interconnections, in the deposition process, which may require several steps. The elimination of wire bonds and package parasitics can result in multioctave bandwidths at microwave and even millimeter wave frequencies.

Downloaded from Digital Engineering Library @ McGraw-Hill (www.digitalengineeringlibrary.com)
Copyright © 2004 The McGraw-Hill Companies. All rights reserved.
Any use is subject to the Terms of Use as given at the website.

RADIO-FREQUENCY AMPLIFIERS AND OSCILLATORS

Monolithic circuits have been implemented using silicon bipolar technology at frequencies below 4 GHz. Because gallium arsenide metal-semiconductor field-effect transistor (MESFET) performance is superior at high frequencies, MMICs are usually designed on GaAs.

Generally, only 5 percent of a monolithic chip is used for active devices. As device yields are low and processing costs are high, the monolithic approach is expensive. Currently it is economical only when very high quantities are needed or when multioctave bandwidth or millimeter wave frequency operation is required, beyond what can be achieved with an HIC.

TUNNEL-DIODE AMPLIFIERS

Chang S. Kim

Introduction

Tunnel-diode (TD) amplifiers are one-port negative-conductive devices. Hence the problems associated with them are quite different from those encountered in conventional amplifier design. Circuit stabilization and isolation between input and output terminals are primary concerns in using this very wide-frequency-range device.

Although there are several possible amplifier configurations, the following discussion is limited to the most practical design, which uses a circulator for signal isolation. The advantage of the circulator-coupled form of tunnel-diode amplifier resides in the fact that it is thereby possible to convert a bilateral one-port amplifier into an ideal unilateral two-port amplifier. Tunnel diodes can provide amplification at microwave frequencies with a relatively simple structure and at a low noise figure.

Tunnel Diodes

Three kinds of tunnel diodes are available, namely, those using Ge, GaAs, and GaSb. *V-I* characteristics and corresponding small-signal conductance-voltage relationships are shown in Figs. 11.3.22 and 11.3.23, respectively. A typical small-signal tunnel-diode equivalent circuit is shown in Fig. 11.3.24. Here g_j, C_j, r_s, L, and C_p are the small-signal conductance, junction capacitance, series resistance, series inductance, and shunt capacitance, respectively. Noise generators e_s and i_j are included for subsequent discussion.

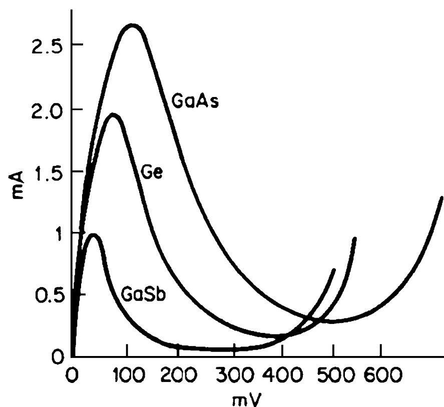

FIGURE 11.3.22 Characteristics of tunnel diodes.

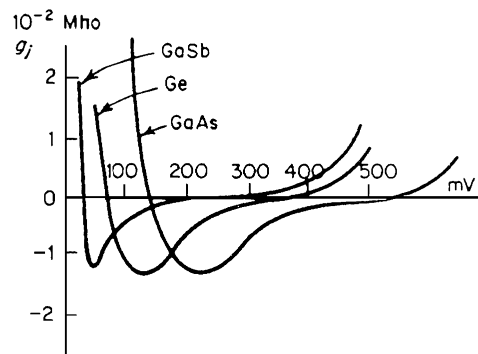

FIGURE 11.3.23 Voltage-vs.-g_j characteristics of tunnel diodes of Fig. 11.3.22.

Downloaded from Digital Engineering Library @ McGraw-Hill (www.digitalengineeringlibrary.com)
Copyright © 2004 The McGraw-Hill Companies. All rights reserved.
Any use is subject to the Terms of Use as given at the website.

RADIO-FREQUENCY AMPLIFIERS AND OSCILLATORS

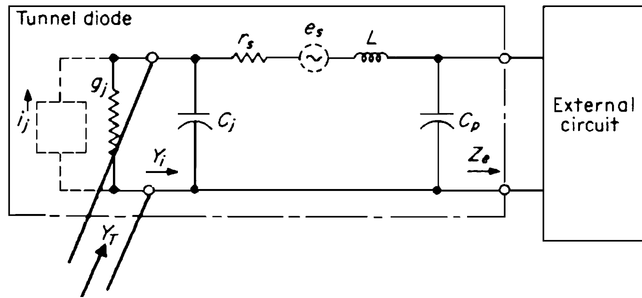

FIGURE 11.3.24 Small-signal equivalent circuit of tunnel-diode amplifier.

Stability

The stability criteria are derived from the immittance expression across the diode terminals and are quite complicated.

Using the short-circuit stable condition, the stability criteria can be simplified considerably. With reference to Fig. 11.3.24, with the external circuit connected, the total admittance Y_T across g_j can be expressed as

$$Y_T(s) = Y_i(s) - g_j = p(s)/q(s)$$

where $Y_i(s)$, the admittance facing g_j, is a positive real function. Since Y_i is connected in parallel with a short-circuit stable device with negative conductance g_i, Y_T is short-circuit-stable. This implies that, since $q(s)$ is always a Hurwitz polynomial, the stability condition is that $p(s)$ must also be Hurwitz polynomial.

A simple graphical interpretation of this stability condition is as follows. The plot* of $Y_T(\omega)$ can be obtained from the plot of $Y_i(\omega)$ by shifting the imaginary axis by $|g_j|$ along the real axis, as shown in Fig. 11.3.25. Since $q(s)$ has no roots in the right half plane, any encirclement of the origin of $Y_T(\omega)$ must come from the right-half-plane roots of $p(s)$ only. Therefore, the circuit will be stable if and only if $Y_T(\omega)$ does not encircle the origin (Fig. 11.3.25*a*). If g_j becomes large so that the origin is encircled by $Y_T(\omega)$ (Fig. 11.3.25*b*), the circuit is unstable.

Tunnel-Diode-Amplifier Design

A simplified block diagram of a circulator-coupled TD amplifier is shown in Fig. 11.3.26. The three basic circuit parts are the tunnel diode, the stabilizing circuit, and the tuning circuit, which includes a four-port circulator. The following conditions are imposed on the amplifier design:

1. In the band
  a. $G_i = \text{Re } Y_i$ is slightly larger than $|g_j|$.
  b. G_i is contributed by the tuning circuit only.
  c. $B_i = \text{Im } Y_i = 0$ at the center frequency f_0 and small in the band.

2. Outside the band
  a. $G_i = \text{Re } Y_i$ is larger than $|g_j|$
  b. If $G_i \leq |g_j|$, B_j should not be zero.

To satisfy these conditions, a stabilizing circuit, shown in Fig. 11.3.26, is required. This circuit is designed so that the following relationships are satisfied:

$$Y_1(f_0) = Y_1(3f_0) = Y_2(f_0) = 0 \qquad Y_1(2f_0) = Y_1(4f_0) = Y_2(3f_0) = 1/\text{R} \qquad Y_s = Y_1 + Y_2$$

where f_0 is the center frequency.

*Here, the plot of $YT_T(\omega)$ represents the case of $Z_e(\omega)$ short-circuited; however, similar plots can be obtained for more general cases.

Downloaded from Digital Engineering Library @ McGraw-Hill (www.digitalengineeringlibrary.com)
Copyright © 2004 The McGraw-Hill Companies. All rights reserved.
Any use is subject to the Terms of Use as given at the website.

RADIO-FREQUENCY AMPLIFIERS AND OSCILLATORS

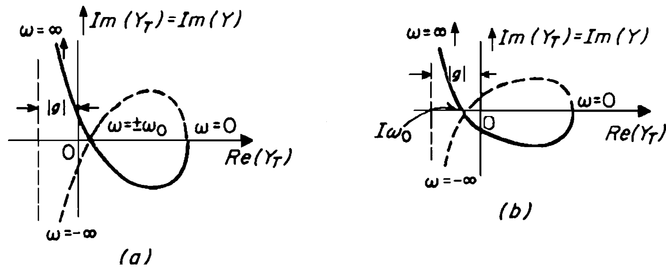

FIGURE 11.3.25 Representative plots of real and imaginary parts of Y_T: (*a*) stable condition; (*b*) unstable condition.

The equivalent circuit of Fig. 11.3.24 can be transformed into the parallel equivalent circuit of Fig. 11.3.27. The following identities relate the parameters of Figs. 11.3.24 and 11.3.27:

$$g_{jp} = 1/|Z_s|^2\, g_j X \qquad g_{sp} = r_s/|Z_s|^2$$

$$B = \omega C_p - \frac{\omega L - (1 - 1/X)1/\omega C_j}{|Z_s|^2} \qquad \text{where } X = 1 + \omega^2 c_j^2/g_j^2$$

$$|Z_s|^2 = \gamma_s - 1/|g_j|X + [\omega L - (1 - 1/X)1/\omega C_j]^2$$

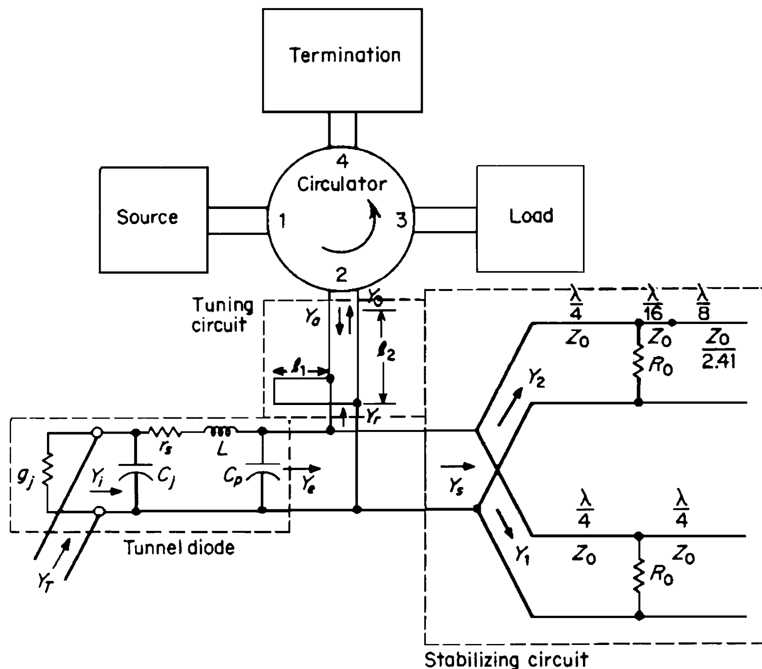

FIGURE 11.3.26 Tunnel-diode amplifier using circulator.

Downloaded from Digital Engineering Library @ McGraw-Hill (www.digitalengineeringlibrary.com)
Copyright © 2004 The McGraw-Hill Companies. All rights reserved.
Any use is subject to the Terms of Use as given at the website.

RADIO-FREQUENCY AMPLIFIERS AND OSCILLATORS

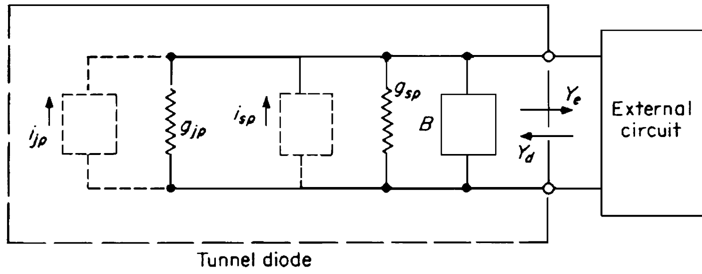

FIGURE 11.3.27 Parallel version of equivalent circuit of Fig. 11.3.24.

The gain can be expressed by

$$|\Gamma|^2 = \left|\frac{Y_e - Y_d}{Y_e + Y_d}\right|^2 \qquad |\Gamma|^2_{f=f_0} = \left|\frac{G_e - g_{sp} + |g_{jp}|}{G_e + g_{sp} - |g_{jp}|}\right|^2$$

where $B_e - B = 0$ at $f = f_0$, in which B_e is the reactive part of Y_e.

In this case, the tuning circuit is a more general matching circuit using combinations of parallel and series transmission lines. It should be noted that $|\Gamma|$ becomes 1, or $g_{sp} = |g_{jp}|$, as the operating frequency increases to f_r, the resistive cutoff frequency, which is defined by

$$f_r = \frac{|g_j|}{2\pi C}\sqrt{1 - \frac{1}{r_s|g_j|}}$$

It is desirable to have a device with f_r several times (at least three) larger than f_0. Furthermore, it is desirable to make the self-resonance frequency f_x,

$$f_x = \frac{1}{2\pi}\sqrt{\frac{1}{LC_j} - \left(\frac{g_j}{C_j}\right)^2}$$

as high as possible (higher than f_c) to improve the stability margin.

The gain expression can be modified to include the input amplifier admittance Y_a of Fig. 11.3.26 as follows:

$$|\Gamma|^2 = \left|\frac{Y_0 - Y_a}{Y_0 + Y_a}\right|^2$$

Similarly, the bandwidth can be determined from the expression for Γ^2 and f_x, above.

Typical germanium tunnel-diode parameters pertinent to S-, C-, and X-band amplifiers with approximate gains to 10 dB are shown in Table 11.3.2.

Noise Figure in TD Amplifiers

A noise equivalent circuit can be completed by inserting a current generator, $\overline{i_j^2}$ and a voltage generator $\overline{e_s^2}$, as shown in Fig. 11.3.24 (dotted lines). The mean-square values are determined from

$$\overline{i_j^2} = 2eI_{eq}\Delta f \qquad \overline{e_s^2} = 2KTr_s\Delta f$$

where I_{eq} = equivalent shot-noise current = I_{dc} = dc current in negative-conductance region.

Downloaded from Digital Engineering Library @ McGraw-Hill (www.digitalengineeringlibrary.com)
Copyright © 2004 The McGraw-Hill Companies. All rights reserved.
Any use is subject to the Terms of Use as given at the website.

TABLE 11.3.2 Typical Germanium Tunnel-Diode Parameters

	S band	C band	X band
$\lvert r_j \rvert = 1/g_j$, Ω	70	70	70
C_j, pF	<1	<0.5	<0.2
L, H	<0.1	<0.1	<0.2
r_s, Ω	$<0.1r_j$	$<0.1r_j$	$<0.1r_j$

The noise equivalent circuit of Fig. 11.3.24 can be transformed into a parallel-equivalent circuit of Fig. 11.3.27 having current generators $\overline{i^2_{jp}}$ and $\overline{i^2_{sp}}$ (dotted lines); $\overline{i^2_{jp}}$ and $\overline{i^2_{sp}}$ can be derived from the two equivalent circuits to be

$$\overline{i^2_{jp}} = 4KT(G_{eq}/|g_j|)|g_{jp}|\Delta f \qquad \overline{i^2_{sp}} = 4KTg_{sp}\Delta f$$

where $G_{eq} = eI_{eq}/2KT = 20I_{eq}$ at room temperature.

Tunnel diodes provide good noise performance with a relatively simple amplifier structure requiring only a dc source for bias. It is therefore a useful low-noise, small-signal amplifier for microwave applications.

PARAMETRIC AMPLIFIERS

Conrad E. Nelson

Introduction

The term *parametric amplifier* (paramp) refers to an amplifier (with or without frequency conversion) using a nonlinear or time-varying reactance. Development of low-loss variable-capacitance (varactor) diodes resulted in the development of varactor-diode parametric amplifiers with low noise figure in the microwave frequency region. Types of paramps include one-port, two-port (traveling-wave), degenerate (pump frequency twice the signal frequency), nondegenerate, multiple pumps, and multiple idlers. The most widely used amplifier is the nondegenerate one-port paramp with a circulator, because it achieves very good noise figures without undue circuit complexity.

One-Port Paramp with Circulator

The one-port paramp with circulator is illustrated in Fig. 11.3.28, and the simplified circuit diagram is shown in Fig. 11.3.29. The input signal and the amplified output signal (at the same frequency) are separated by the circulator. The cw pump source is coupled to a back-biased varactor to drive the nonlinear junction capacitance at the pump frequency. The signal and pump currents mix in the nonlinear varactor to produce voltages at many frequencies. The additional (idler) filter allows only the difference or idler current to flow at the idler frequency; i.e.,

$$f_i = f_p - f_s$$

The idler current remixes with the pump current to produce the signal frequency again. The phasing of this signal due to nonlinear reactance mixing is such that the original incident signal is reenforced (i.e., amplified) and reflected back to the circulator. The one-port paramp at band center is essentially a negative-resistance device at the signal frequency.

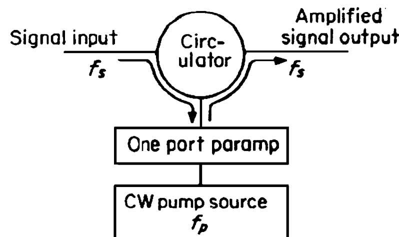

FIGURE 11.3.28 One-port parametric amplifier and circulator.

Downloaded from Digital Engineering Library @ McGraw-Hill (www.digitalengineeringlibrary.com)
Copyright © 2004 The McGraw-Hill Companies. All rights reserved.
Any use is subject to the Terms of Use as given at the website.

RADIO-FREQUENCY AMPLIFIERS AND OSCILLATORS

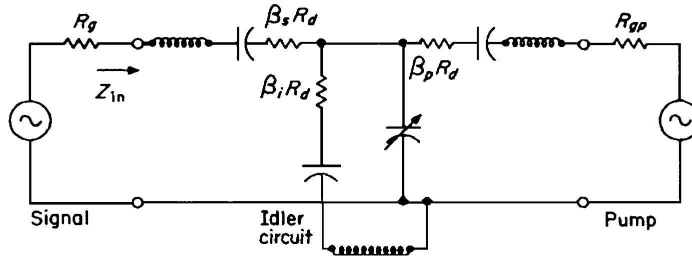

FIGURE 11.3.29 Circuit of one-port paramp using single-tuned resonators.

Power Gain and Impedance Effects

The one-port paramp power gain at the signal frequency is

$$G = \left| \frac{Z_{\text{in}} - R_g}{Z_{\text{in}} + R_g} \right|^2$$

where R_g is the signal-circuit equivalent generator resistance and Z_{in} is the input impedance at the signal frequency.

For a single-tuned signal circuit and a single-tuned idler circuit the input impedance at the signal frequency is

$$Z_{\text{in}} = \beta_s R_d + jX_s - \frac{\sigma \beta_s \beta_i R_d^2}{\beta_i R_d - jX_i} \quad \text{where } \sigma = \frac{m_1^2 f_c^2}{\beta_s \beta_i f_s f_i}$$

The diode loss resistance R_d has been modified at the signal and idler frequencies to include circuit losses (that is, $\beta \geq 1$). The signal and idler reactances are X_s and X_i, respectively, and must include the varactor junction capacitance. (In the simplified circuit the diode package capacitance has been neglected.) For a fully pumped varactor the cutoff frequency is

$$f_c = 1/2\pi R_d C_R$$

where C_R is the junction capacitance at reverse breakdown. The modulation ratio m_1 for an abrupt-junction diode is 0.25.

Bandwidth and Noise

Factors that determine the overall paramp bandwidth include the varactor characteristics (cutoff frequency, junction and package capacitance, and lead inductance), choice of idler (pump) frequency, the nature of the signal and idler resonant circuits and the choice of band-center gain. Multiple-tuned signal and idler circuits are often used to increase the overall paramp bandwidth.

At band center the effective noise temperature of the one-port paramp (due to the diode and circuit loss resistances at the signal and idler frequencies) is

$$T_e = T_d \frac{G-1}{G} \left(\frac{f_p}{f_i} \frac{\sigma}{\sigma - 1} - 1 \right)$$

Downloaded from Digital Engineering Library @ McGraw-Hill (www.digitalengineeringlibrary.com)
Copyright © 2004 The McGraw-Hill Companies. All rights reserved.
Any use is subject to the Terms of Use as given at the website.

where T_d is the temperature of varactor junction and loss resistances. The effective noise temperature can be reduced by cooling the paramp below room temperature and/or by proper choice of pump frequency. Circulator losses must be included when determining the overall paramp noise figure.

Pump Power

The pump power required at the diode to fully drive a single varactor is

$$P_p = k_l \beta_p R_d [\omega_p C_R (\phi - V_R)]^2 \quad \text{(watts)}$$

where the pump circuit loss resistance and diode resistance = $\beta_p R_d$, and $k_1 = 0.5$ for an abrupt-junction varactor.

Gain and Phase Stability

The stability of the cw pump source (amplitude and frequency) is a significant factor in the overall paramp gain and phase stability. For small pump-power changes an approximate expression for the paramp power-gain variation is

$$\frac{\Delta G}{G} \approx \frac{G-1}{\sqrt{G}} \frac{\Delta P_p}{P_p}$$

Environmental temperature changes often require a temperature-regulated enclosure for the paramp and pump source.

At low levels of nonlinear distortion, the amplifier third-order relative power intermodulation product at band center is a function of the one-port amplifier gain and the incident signal power level; i.e.,

$$\Delta(\text{IMP}) \propto \frac{(G-1)^4 P_s^2}{G} \approx G^3 P_s^2 \approx G P_{\text{out}}^2$$

Thus low-band-center amplifier gains reduce this nonlinear distortion.

MASER AMPLIFIERS

Gunter K. Wessel

Introduction

A *maser* is a microwave active device whose name is an acronym derived from microwave amplification by stimulated emission of radiation. A *laser* is an amplifier or oscillator also based on stimulated emission but operating in the optical part of the spectrum. The expressions microwave, millimeter, submillimeter, infrared, optical, and ultraviolet maser are also in common use. Here the word maser is used for the whole frequency range of devices, the *m* standing for molecular.

A description of the laser principle, some of its properties and means of achieving laser operations, is given in Sec. 9.

In these devices, no tubes or transistors are employed in the radiation process, but the properties of atoms or molecules—as gases, liquids, or solids—serve for the amplification of the signals. Oscillators require the addition of a feedback mechanism. The interaction of the electromagnetic radiation with the maser material occurs in a suitable cavity or resonance structure. This structure often serves the additional purpose of generating a desired phase relationship between different spatial parts of the signal. The application of external energy, required for the amplification or oscillation process, is referred to as *pumping*. The pumping power consists, in many cases, of external electromagnetic radiation of a different frequency (usually higher) from that for the signal.

Downloaded from Digital Engineering Library @ McGraw-Hill (www.digitalengineeringlibrary.com)
Copyright © 2004 The McGraw-Hill Companies. All rights reserved.
Any use is subject to the Terms of Use as given at the website.

RADIO-FREQUENCY AMPLIFIERS AND OSCILLATORS

Microwave masers are used as low-noise preamplifiers and as time and frequency standards. The stimulated emission properties of atoms and molecules at optical frequencies, with their relatively high noise content, make the laser more useful for high-power light amplification and oscillation.

Maser Principles

In the processes of emission and absorption, atoms or molecules interact with electromagnetic radiation. It is assumed that the atoms possess either sharp internal-energy states or broader energy bands. A change of internal energy from one state to another is accompanied by absorption or emission of electromagnetic radiation, depending on the direction of the process. The difference in energy from the original to the final state is proportional to the frequency of the radiation, the proportionality constant being Planck's constant h.

The processes of the spontaneous emission and absorption were defined by Einstein.

Spontaneous emission:

$$-\frac{dN_2}{dt} = A_{21}N_2 \tag{1}$$

Absorption:

$$-\frac{dN_1}{dt} = B_{12}\mu(v_{12},T)N_1 \tag{2}$$

where N_1 and N_2 are population densities of atoms or molecules of material having energy states E_1 and E_2 and an energy separation $E_2 - E_1 = hv_{12}$ between them, and A_{21} and B_{12} are the Einstein coefficients.

At high temperature, an inconsistency in the equilibrium system arises unless a second emission process, stimulated emission, takes place. The rate of stimulated emission is defined very similarly to that of absorption (the stimulated emission is sometimes called *negative absorption*):

$$-\frac{dN_2}{dt} = B_{21}\mu(v_{12},T)N_2 \tag{3}$$

In temperature equilibrium, the rates of emission must be equal to the rate of absorption

$$A_{21}N_2 + B_{21}\mu N_2 = B_{12}\mu N_1 \tag{4}$$

Assuming that the ratio of the population densities is equal to the Boltzmann factor,*

$$N_1/N_2 = \exp\,(hv_{12}/kT) \tag{5}$$

Equation (4) yields, for the radiation density,

$$\mu(v_{12},T) = \frac{A_{21}/B_{21}}{B_{12}/B_{21}\exp\,(hv_{12}/kT) - 1} \tag{6}$$

Equation (6) is identical with Planck's radiation law if we set

$$B_{12} = B_{21} \tag{7a}$$

and

$$A_{21}/B_{21} = 8\pi hv_{12}^3/c^3 \tag{7b}$$

where c is the velocity of light.

Equation (7*a*) shows the close relationship between stimulated emission and absorption. The rates of population decrease, for these two processes [Eqs. (2) and (3)] depend only on their respective population densities.

*It is assumed that the statistical weights are equal to 1.

Downloaded from Digital Engineering Library @ McGraw-Hill (www.digitalengineeringlibrary.com)
Copyright © 2004 The McGraw-Hill Companies. All rights reserved.
Any use is subject to the Terms of Use as given at the website.

RADIO-FREQUENCY AMPLIFIERS AND OSCILLATORS

Neglecting the spontaneous emission, the net absorption or the net stimulated emission of an incoming radiation depends, therefore, only on the difference in population density: for absorption, if $(N_1 - N_2) > 0$; for amplification, if $(N_1 - N_2) < 0$. In particular, if a system is in quasiequilibrium such that the upper energy state E_2 is more populated than the lower one, E_1, it is capable of amplifying electromagnetic radiation.

To create and maintain the quasiequilibrium requires application of external energy since the natural equilibrium has the opposite population excess $(N_1 > N_2)$. Different masers differ widely in the methods of how to accomplish the reverse in population density.

Properties of Masers

The properties of masers can be understood by analyzing Eqs. (1) to (7*b*), as follows.

Signal-to-Noise Ratio. From Eqs. (1) and (3) it follows that the Einstein coefficients A and B have different dimensions but the ratio $B_{21}\mu/A_{21}$ is dimensionless. Here μ is proportional to the strength of the incoming signal and $B_{21}\mu$ is proportional to the amplified signal strength. A_{21} is proportional to the noise contribution because of spontaneous emission. After rewriting Eq. (7*b*),

$$B_{21}\mu/A_{21} = c^3\mu/8\pi h v_{12}^3 \tag{8}$$

the ratio is found to be proportional to the signal-to-noise ratio of the amplifier. It thus becomes clear that the noise contribution (thermal or Johnson noise) is very small at microwave frequencies, whereas it becomes very large at optical frequencies (an increase of 15 orders of magnitude for an increase of 5 orders for the frequency). Microwave masers are therefore very useful as low-noise microwave preamplifiers.

Infrared, optical, and ultraviolet masers (lasers), on the other hand, are commonly used for power amplification and as powerful light sources (oscillators). The high content of spontaneous-emission noise does not make them easily applicable for low-noise amplification or sensitive detection of light, except in a few special cases.

Linearity and Line Width

The proportionality between the incoming signal strength, the radiation density μ, and the amplified signal strength means that a maser is a linear amplifier as long as it is not driven into saturation. The latter occurs when the excess population becomes $N_2 - N_1 \approx N_2$.

Line Width. In the absence of a strong interaction of the individual atoms of the material, either with the environment or with each other, the line width is determined by the average length of time of interaction of an atom with the radiation field. However, if regeneration because of feedback is taking place, the line width may be much narrower because of the following effect. It is assumed that the incoming radiation has a frequency distribution, as shown in Fig. 11.3.30. The amplified signal is proportional to the rate of stimulated emission dN_2/dt. According to Eq. (3), the latter is proportional to $\mu(v_{12})$. Thus the center portions of the line will be more amplified than the wings, leading to increasingly narrower line widths. In an oscillator the final width is ultimately limited by statistical fluctuations because of the quantum nature of the radiation.

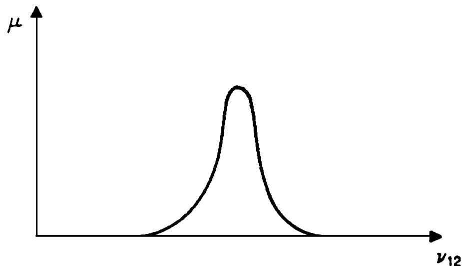

FIGURE 11.3.30 Frequency distribution of radiation incoming to maser.

The narrow line width coupled with the low-noise property of a microwave maser makes the latter useful as a time and frequency standard device. To reduce interaction, gases are used as microwave maser materials.

In low-noise microwave amplifiers one is usually interested in a relatively large bandwidth (typically 50 MHz or more). For such amplifier solid-state materials are used, with strong spin-spin interactions of atoms (for example, Cr^{3+} in ruby).

Downloaded from Digital Engineering Library @ McGraw-Hill (www.digitalengineeringlibrary.com)
Copyright © 2004 The McGraw-Hill Companies. All rights reserved.
Any use is subject to the Terms of Use as given at the website.

RADIO-FREQUENCY AMPLIFIERS AND OSCILLATORS

Tuning

Solid-state microwave masers can be tuned over a wide range of frequencies by adjustment of an external magnetic field, while the relative tuning range by a magnetic field is smaller by a factor of 10^{-4} to 10^{-5} in optical masers. Generally, in lasers, one has to depend on fixed frequencies wherever a suitable spectral line occurs in the material; however, modern liquid-dye lasers can be tuned over a relatively wide range in the visible spectrum.

Power Output

The power output owing to stimulated emission depends on the number of excess atoms $(N_2 - N_1)$ available for the transition. Assuming p to be the probability of a transition per second, the power output is given by

$$P = (N_2 - N_1)hv_{12}p \tag{9}$$

Equation (9) shows that the power output of a microwave gas maser must be very low (for example, 100 to 1 pW) because the population density and the frequency are small. On the other hand, solid-state lasers and some gas lasers with very high efficiencies may have cw power outputs of 1000 W and more.

Coherence

The similarity between absorption and stimulated emission [as expressed in Eqs. (2), (3), and (7*a*)] means that the stimulated emission is a coherent process. In practice, this means that a beam of radiation will be amplified only in the direction of propagation of the incoming beam and when all atoms participate coherently in the amplification. This is very different from the noise-producing spontaneous emission, where the radiation is emitted isotropically and no phase relationship exists between the radiation coming from different atoms.

The coherence of the stimulated emission enables one to produce coherent light and radiation patterns similar to those which are well known and applied in the radio and microwave parts of the spectrum. In particular, it is possible by a suitable geometry of the device to produce a plane-parallel light beam whose divergence angle is limited only by diffraction. The divergence angle is given by

$$\alpha \approx \lambda/d \tag{10}$$

Time and Frequency Standards

The ammonia and hydrogen atomic-beam masers are used as time and frequency standards with operating frequencies of about 24 GHz and about 1.4 GHz, respectively. The reverse of population difference is achieved by focusing atoms in the excited state into a suitable microwave cavity, whereas the atoms in the lower state are defocused by a special focuser and do not reach the interior of the cavity. The microwave field in the cavity causes stimulated emission and amplification. If the cavity losses can be overcome, oscillations will set in. Time and frequency accuracy of 1 part in 10^{12} or higher can be obtained with modern maser standard devices.

Three- and Four-Level Devices

In many of the masers of all frequency regions, population reverse is obtained by a *three-level-maser* method first described by Bloembergen. Radiation from an external power source at the pumping frequency v_p (Fig. 11.3.31) is applied to the material. E_3 may be a band to make the pumping more economical. The material is contained in a suitable cavity, a slow-wave structure, or other resonance structure which is resonant at the signal frequency v_s. Under favorable conditions of the pumping power, the frequency ratio v_s/v_p, and the involved relaxation times, an excess population in the excited state E_2 over the ground state E_1 can be obtained. The interaction with the electromagnetic field of frequency v_s causes stimulated emission. Thus amplification (and if required, oscillation) is produced.

Downloaded from Digital Engineering Library @ McGraw-Hill (www.digitalengineeringlibrary.com)
Copyright © 2004 The McGraw-Hill Companies. All rights reserved.
Any use is subject to the Terms of Use as given at the website.

RADIO-FREQUENCY AMPLIFIERS AND OSCILLATORS

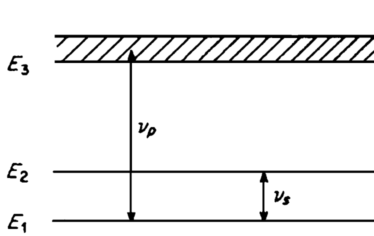

FIGURE 11.3.31 Three-level maser.

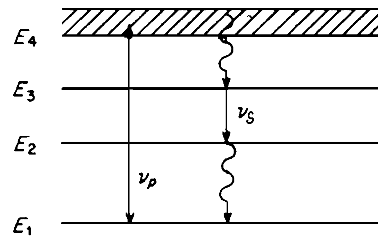

FIGURE 11.3.32 Four-level maser.

The four-level maser (Fig. 11.3.32) percent has the additional advantage that the population of the ground state does not have to be reduced to less than 50 percent of its original equilibrium value and the level E_4 can remain a relatively wide band. The transfer of energy from E_4 to E_1, and E_2 to E_1, is by spontaneous decay or some other means like spin-lattice relaxation. Most solid-state microwave and optical masers are of the three- or four-level variety.

Semiconductor Lasers

Stimulated light emission can be obtained by carrier injection in certain semiconductor materials. Upon application of an external dc potential, recombination light emission can take place at the interface of an *n*- and *p*-type semiconductor (for example, Zn and Te in GaAs). The semiconductor laser requires only a very simple power source (a few volts of direct current). However, the laser material has to be cooled to liquid-nitrogen temperature and the power output is relatively low.

Applications

The particular properties of devices based on stimulated emission have resulted in numerous applications which often surpass the capabilities of standard devices. In some instances, e.g., holography, new fields have opened up through the emergence of lasers and masers.

Solid-state microwave preamplifiers for communication, radar, and radio astronomy have by far the best signal-to-noise ratio of all microwave amplifiers. The hydrogen-beam maser is the most accurate of all frequency and time standards.

Lasers have revolutionized the field of optical instrumentation and spectroscopy. They have made possible the new field of nonlinear optics. The laser is or may be used in many applications where large energy densities are required, as in microwelding, medical surgery, or even in cracking rocks in tunnel building. Lasers can be used as communication media where extremely large bandwidths are required. Optical radar, with its high precision owing to the short wavelength, uses lasers as powerful, well-collimated light sources. Their range extends as far as the moon.

ACOUSTIC AMPLIFIERS

Stephen W. Tehon, Y. J. Lin, Wen-Chung. Wang

Acoustoelectric Interaction

The acoustic amplifier stems from the announcement by Hutson, McFee, and White, in 1961, that they had observed a sizable influence on acoustic waves in single crystals of CdS caused by a bias current of change carriers. CdS is both a semiconductor and piezoelectric crystal, and the interaction was found to involve an

Downloaded from Digital Engineering Library @ McGraw-Hill (www.digitalengineeringlibrary.com)
Copyright © 2004 The McGraw-Hill Companies. All rights reserved.
Any use is subject to the Terms of Use as given at the website.

RADIO-FREQUENCY AMPLIFIERS AND OSCILLATORS

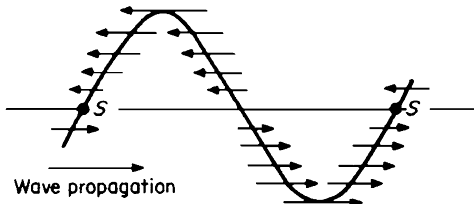

FIGURE 11.3.33 Traveling wave of electric field intensity induced by traveling stress wave.

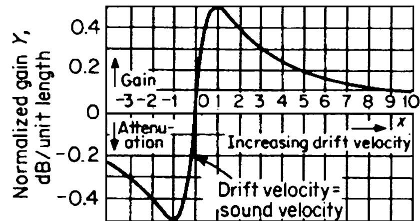

FIGURE 11.3.34 Normalized gain as a function of bias field.

energy transfer via traveling electric fields generated by acoustic waves, producing, in turn, bunching of the drift carriers. Quantitative analyses showing that either loss or gain in wave propagation could be selected by controlling the drift field were published by White.

Figure 11.3.33 illustrates the nature of the interaction. As an acoustic wave propagates in the crystal its stresses induce a similar pattern of electric field through piezoelectric coupling. Since the coupling is linear, compressive stresses in half the wave induce a forward-directed field, and tensile stresses in the remainder of the wave induce a backward-directed field. Drifting charge carriers tend to bunch at points of zero field to which they are forced by surrounding fields. When a charge carrier loses velocity in bunching, it gives its excess kinetic energy to the acoustic wave; when it gains velocity, it extracts energy from the wave. Therefore the drift field is effective for determining attenuation or amplification in the range near which carriers move at the speed of sound. Figure 11.3.34 illustrates the gain characteristic as a function of drift velocity. At the zero-crossover point, the carrier velocity is just equal to the velocity of propagation for the acoustic wave; the gain ranges from maximum attenuation up to maximum amplification over a relatively small change in bias. Beyond this range of drift velocity, bunching becomes decreasingly effective, and the interaction has less effect on the acoustic wave.

Piezoelectric Materials

Piezoelectricity is the linear, reversible coupling between mechanical and electric energy because of displacement of charges bound in molecular structure. Pressure applied to a piezoelectric material produces a change in observed surface density of charge, and conversely, charge applied over the surfaces produces internal stress and strain. If S is the strain, T the stress, E the electric field intensity, and D the dielectric displacement, the piezoelectric effect at a point in a medium is described by the pair of linear equations

$$S = sT + dE \qquad D = dT + \epsilon E$$

where constant s = elastic compliance
ϵ = permittivity
d = piezoelectric constant

The ratio $d^2/s\epsilon$, calculated from these constants for a particular piezoelectric material, is defined as K^2, where K^2 is the coefficient of electromechanical coupling. As a consequence of conservation of energy, it can be shown that K is a number less than unity and that a fraction K^2 of applied energy (mechanical or electric) is stored in the other form (electric or mechanical). Since D and E are vectors and S and T are tensors, the piezoelectric equations are tensor equations and are equivalent to nine algebraic equations, describing three vector and six tensor components.

Materials that are appreciably piezoelectric are either crystals with anisotropic properties or ceramics with ferroelectric properties which can be given permanent charge polarization through dielectric hysteresis. Ferroelectric ceramics, principally barium titanate and lead zirconate titanate, are characterized by relative dielectric constants ranging from several hundred to several thousand, by coupling coefficients as high as 0.7, and by polycrystalline grain structure which will propagate acoustic waves with moderate attenuation at frequencies extending up to the low-megahertz range.

Downloaded from Digital Engineering Library @ McGraw-Hill (www.digitalengineeringlibrary.com)
Copyright © 2004 The McGraw-Hill Companies. All rights reserved.
Any use is subject to the Terms of Use as given at the website.

Single crystals are generally suited for much higher acoustic frequencies, and in quartz acoustic-wave propagation has been observed at 125 GHz. Quartz has low loss but a low coupling coefficient. Lithium niobate is a synthetic crystal, ferroelectric and highly piezoelectric; lithium tantalate is somewhat similar. The semiconductors cadmium sulfide and zinc oxide are moderately low in loss and show appreciable coupling.

Stress Waves in Solids

Acoustic waves propagate with low loss and high velocity (5000 m/s) in solids. Solids also have shear strength, whereas sound waves in gases and fluids are simple pressure waves, manifested as traveling disturbances measurable by pressure and longitudinal motion.

Sound waves in solids involve either longitudinal or transverse particle motion. The transverse waves may be propagation of simple shear strains or may involve bending in flexural waves. Since different modes of waves travel with different velocities, and since both reflections and mode changes can occur at material discontinuities, the general pattern of wave propagation in a bounded solid medium is quite complicated.

Bulk waves are longitudinal or transverse waves traveling through solids essentially without boundaries; e.g., the wavefronts extend over many wavelengths in all directions. A solid body supporting bulk waves undergoes motion and stress throughout its volume. A *surface wave* follows a smooth boundary plane, with elliptical particle motion which is greatest at the surface and drops off so rapidly with depth that almost all the energy is carried in a one-wavelength layer at the surface.

Ideally, the wave medium for surface-wave propagation is regarded as infinitely deep; practically if it is many wavelengths deep, its properties are equivalent. A surface wave following a surface free from forces is a Rayleigh wave; if an upper material with different elastic properties bounds the surface, the motion may be a Stonely wave.

Bulk-Wave Devices

Most acoustic amplifiers utilizing bulk waves have the components shown in Fig. 11.3.35. The input and output transducers are piezoelectric crystals or deposited thin layers of piezoelectric material, used for energy conversion at the terminals. The amplifier crystal is generally CdS, which is not only piezoelectric but also an *n*-type semiconductor. Electrodes are attached at the input and output surfaces of the CdS crystal, for bias current. Since the mobility of negative-charge carriers in CdS is only about 250 $cm^2/V \cdot s$, large bias fields are required to provide a drift velocity equal to acoustic velocity: in CdS, 4500 m/s for longitudinal waves and 1800 m/s for shear waves. The buffer rods shown in Fig. 11.3.35 are therefore added for electrical isolation of the bias supply. Furthermore, the transducers and amplifying crystal are cut in the desired orientation, to couple to either longitudinal or shear waves.

In the analysis of bulk-wave amplification the crystal properties are characterized by f_D = diffusion frequency = $\omega_D/2\pi$; f_C = dielectric relaxation, or conductivity frequency = $\omega_C/2\pi$; $\gamma = (1 - f)$ times the drift velocity divided by the acoustic phase velocity, where f is the fraction of space charge removed from the conduction band by trapping; k = coefficient of electromechanical coupling; and ω = radian frequency of maximum gain = $\sqrt{\omega_c \omega_d}$. Figure 11.3.36 shows the computed gain curves, using these constants, for four values of drift velocity. The frequency of maximum gain can be selected by control of crystal conductivity, which is

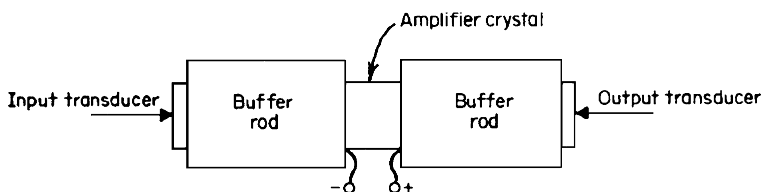

FIGURE 11.3.35 Typical structure for acoustic amplification measurements.

Downloaded from Digital Engineering Library @ McGraw-Hill (www.digitalengineeringlibrary.com)
Copyright © 2004 The McGraw-Hill Companies. All rights reserved.
Any use is subject to the Terms of Use as given at the website.

RADIO-FREQUENCY AMPLIFIERS AND OSCILLATORS

easily accomplished in CdS by application of light. The amount of gain, and to some extent the bandwidth, are controlled by the bias field.

Figure 11.3.37 shows characteristics specifically calculated for CdS with shear acoustic-wave amplification. Large bias voltages (800 to 1300 V/cm) are required, and extremely high gains are possible. Generally, heat dissipation owing to the power supplied by bias is so high (up to 13 W/cm^3 at $\gamma = 0.76$) that only pulsed operation is feasible.

Surface-Wave Devices

The disadvantages in bulk-wave amplifiers, evidenced as excessive bias requirements, could be alleviated if materials with high mobility were available. However, the amplifier crystal must show low acoustic loss, high piezoelectric coupling, and high mobility; a suitable material combining these properties has not been found. Figure 11.3.38 shows an acoustic amplifier structure which operates with acoustic surface waves and provides charge carriers in a thin film of silicon placed adjacent to the insulating piezoelectric crystal. Coupling for the interaction takes place in the electric field across the very small gap between piezoelectric and semiconductor surfaces. Transducers are formed by metallic fingers, interlaced to provide signal field for piezoelectric coupling between adjacent fingers. This interdigital-array technique is flexible, providing means for complicated transducer patterns useful in signal processing.

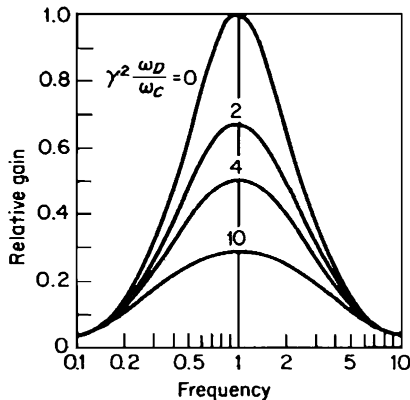

FIGURE 11.3.36 Normalized plots of gain vs. frequency. Note symmetry of frequency response and effects of bias and critical frequency values.

The composite structure makes it possible to combine separate materials, one chosen for strong piezoelectric coupling and the other chosen for high mobility, to cooperatively produce interactive amplification, or attenuation, of acoustic waves propagating in the piezoelectric component. The variety of material combinations and structural modifications possible has given rise to extensive analysis and experimental development in many countries. Lithium niobate crystals have the strongest piezoelectric coupling

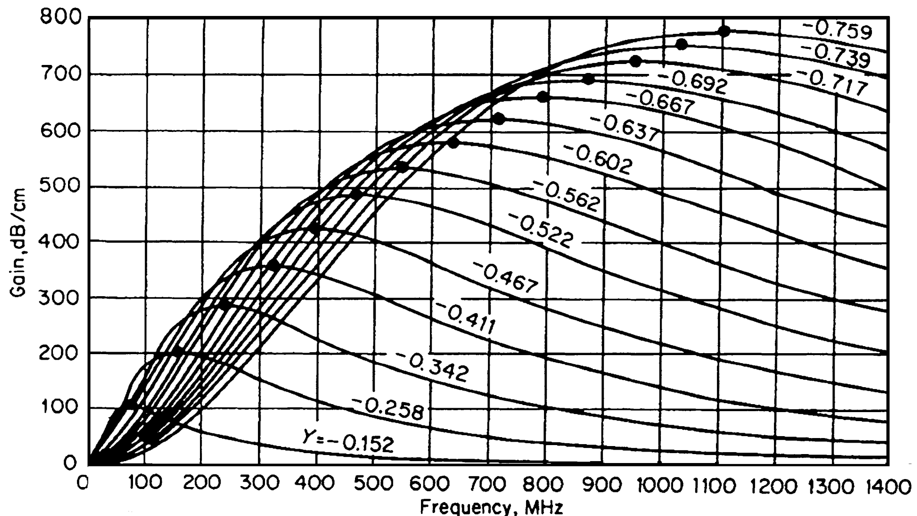

FIGURE 11.3.37 Gain vs. frequency for CdS shear-wave amplification at $f_D = 796$ MHz.

Downloaded from Digital Engineering Library @ McGraw-Hill (www.digitalengineeringlibrary.com)
Copyright © 2004 The McGraw-Hill Companies. All rights reserved.
Any use is subject to the Terms of Use as given at the website.

RADIO-FREQUENCY AMPLIFIERS AND OSCILLATORS

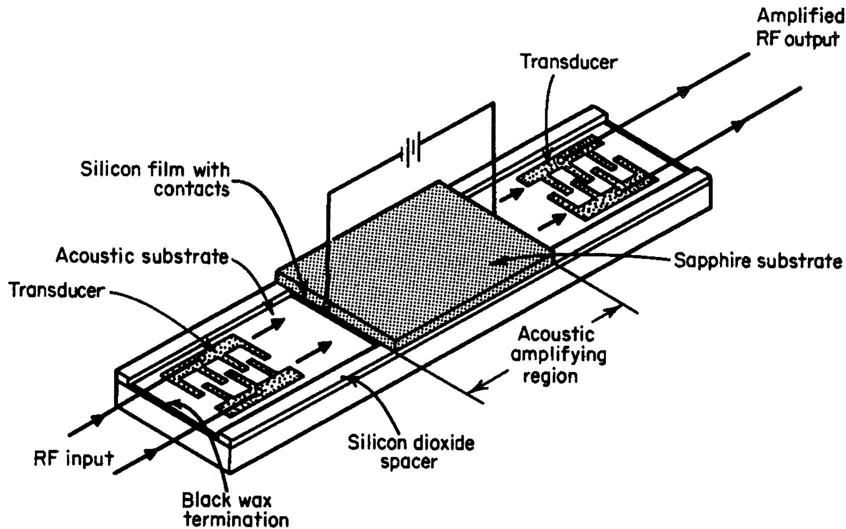

FIGURE 11.3.38 Structure of a surface-wave acoustic amplifier. (See Lakin and Shaw)

of materials acoustically suitable for high-frequency operation, and indium antimonide semiconductor films have the highest drift mobility. Since high-frequency performance requires extremely accurate control of narrow air gaps, amplifier structures employing surface waves that propagate along the interface between a piezoelectric crystal and a deposited semiconductor film have been developed.

Surface-acoustic-wave (SAW) devices, with interdigital transducers designed for wide-band or filter frequency-response characteristics, have values of signal insertion loss owing primarily to acoustic attenuation and to the conversion loss of the input and output transducers. One role of acoustic amplification can be to offset that basic insertion loss. This is illustrated in Fig. 11.3.39, which shows the gain characteristic for a Rayleigh surface-wave amplifier employing lithium niobate, separated by thin dielectric rails from a silicon-on-sapphire semiconductor film. Continuous operation with cw signals is facilitated by the surface-wave geometry, specifically by high-mobility semiconductor films backed by dielectric substrate heat sinks. Amplified signal power, carried by bunched charge carriers, flows in the semiconductor films, so the level of signal saturation is a function of film thickness, compounded by reduction of drift mobility at high temperature. A saturation level of 15 dBm, with cw signals at 340 MHz, has been observed using a 550-Å indium antimonide film 25 μm wide.

Typically, gain in a surface-wave amplifier can be as much as 100 dB in a crystal less than 1 cm long, operating with as much as 50 percent bandwidth at frequencies as high as several hundred megahertz. The amount and direction of gain are controlled by the bias field, in some cases in conjunction with incident optical illumination. The bandwidth and center frequency of the transducers are determined by the geometry of the interdigital arrays. Semiconductor films of silicon or indium antimonide operate at much lower values of bias field than are required in bulk-wave amplifiers and can be deposited on a dielectric substrate in narrow strips to permit parallel excitation at low voltage. The upper frequency limits are set by resolution of the photolithographic processes used to form the transducer fingers and by the ability to provide air gaps, in the Rayleigh wave configurations, of much less than a wavelength. Electron-beam lithography of interdigital arrays has been developed for high resolution, extending transducer technology to more than 3 GHz.

Surface-Acoustic-Wave-Amplifier Analysis

When the SAW amplifier evolved from its bulk wave counterpart, the amplification medium was piezoelectric semiconductor CdS [see White (1967)], and the gain expression was obtained by solving the field equations. Ingebrigtsen (1970 and Lakin and Shaw (1969) were the first ones to investigate the gain of the

Downloaded from Digital Engineering Library @ McGraw-Hill (www.digitalengineeringlibrary.com)
Copyright © 2004 The McGraw-Hill Companies. All rights reserved.
Any use is subject to the Terms of Use as given at the website.

RADIO-FREQUENCY AMPLIFIERS AND OSCILLATORS

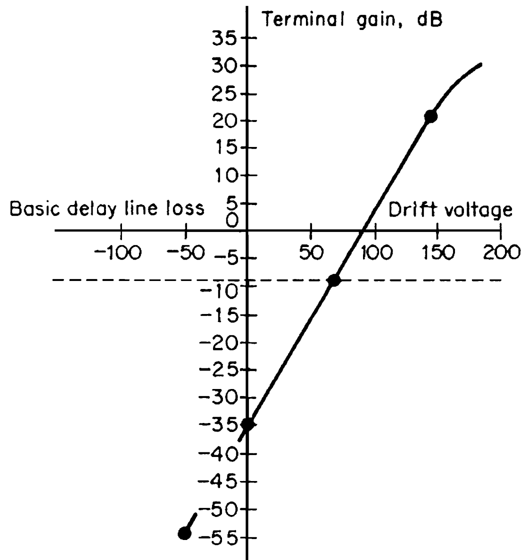

FIGURE 11.3.39 Terminal gain of an air-gap Rayleigh wave amplifier. The semiconductor, Si, was segmented to reduce the required drift voltage. [*After Lakin and Shaw (1969)*]

separate-medium SAW amplifiers by using perturbation techniques. Finally, a general form, similar to the expressions derived by White (1962) for bulk wave amplifiers, is obtained by Kino and Reeder (1971) using normal mode theory. Hunsinger and Datta (1986) introduced the concept of capacitance perturbation into the transmission line model of SAW propagation. This technique has extensively simplified the analytical process. We have further utilized the transmission line model to derive a SAW amplifier gain expression, in which the effects of the passivation and the encapsulation layers are included [see Lin (1995)]. Because of the space limitation, we will present the simplified one-dimensional analysis; however, the result of the two-dimensional analysis for the SAW amplifier will be given.

If we define the surface potential ϕ of a SAW as the voltage V and select the current I to satisfy the power P of the SAW such that $P = VI^*$, then the familiar relationships for a transmission line can be used to describe SAW propagation:

$$V_a = \frac{1}{\sqrt{LC}} \qquad C = \frac{1}{Z_a V_a} \tag{11}$$

where L and C are the distributed inductance and capacitance, both defined by the Mason model, and $V_a = \omega/k$ is the acoustic wave velocity. Z_a, the characteristic impedance of the propagating SAW, is defined as

$$Z_a = \frac{\phi_a \phi_a^*}{2P} \tag{12}$$

where ϕ_a is the electric potential generated by the SAW and P is the total power of that wave. If a layer of charge is placed above the surface of the SAW propagation path, separated by h (see Figs. 11.3.40 and

Downloaded from Digital Engineering Library @ McGraw-Hill (www.digitalengineeringlibrary.com)
Copyright © 2004 The McGraw-Hill Companies. All rights reserved.
Any use is subject to the Terms of Use as given at the website.

RADIO-FREQUENCY AMPLIFIERS AND OSCILLATORS

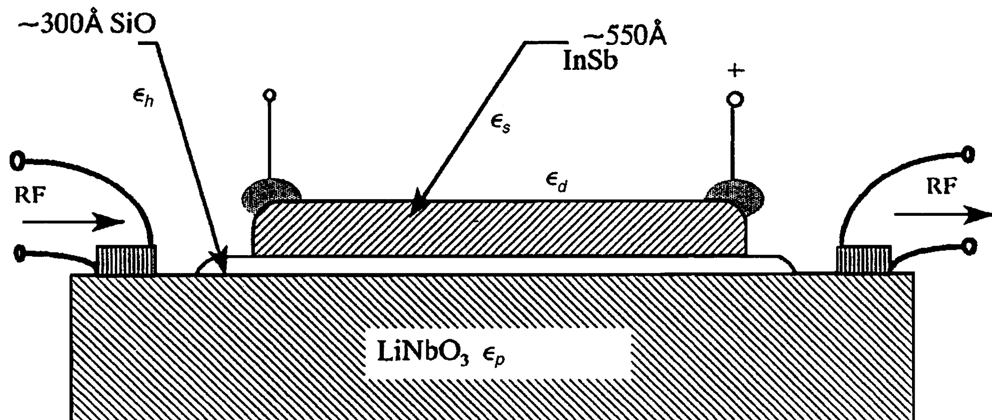

FIGURE 11.3.40 Monolithic acoustic surface-wave amplifier. [*After Coldren and Kino (1971)*]

11.3.41), it is equivalent to have an additional capacitance ΔC on the transmission line, which can be defined as

$$\Delta C = -\frac{\rho_s W}{\phi_{ah}} \tag{13}$$

where ρ_s = induced surface charge
W = beam width
ϕ_{ah} = acoustic potential value at $y = h$, where the charge is located

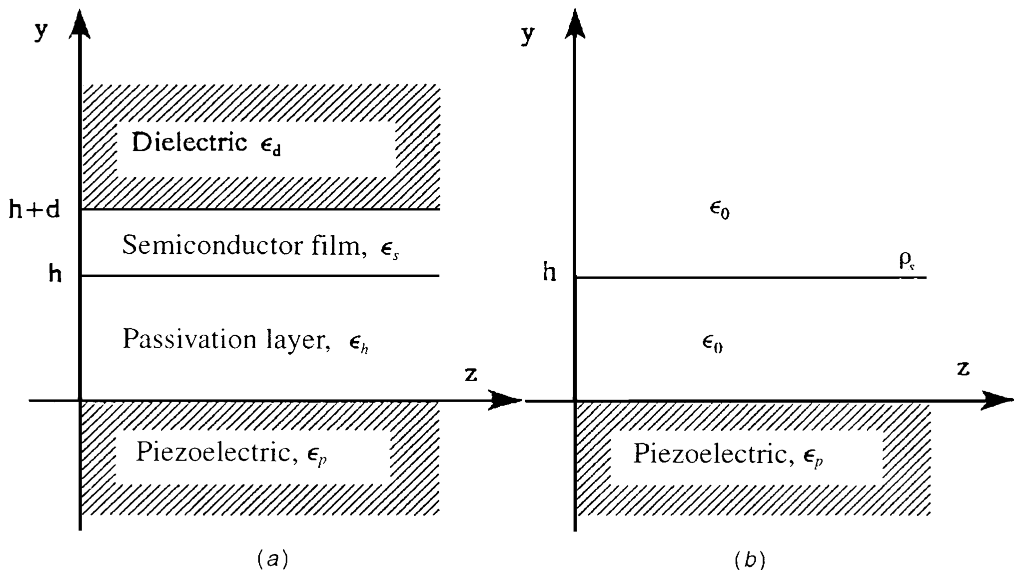

FIGURE 11.3.41 Analytical model: (*a*) two-dimensional semiconductor layer, and (*b*) simplified one-dimensional.

Downloaded from Digital Engineering Library @ McGraw-Hill (www.digitalengineeringlibrary.com)
Copyright © 2004 The McGraw-Hill Companies. All rights reserved.
Any use is subject to the Terms of Use as given at the website.

Because of ΔC, V_a will change accordingly (assume that the SAW propagates as $e^{j(\omega t - kz)}$):

$$\frac{\Delta V_a}{V_a} = -\frac{\Delta k}{k} = -\frac{1}{2}\frac{\Delta C}{C} \tag{14}$$

The imaginary part of Δk ($\Delta k = \beta + j\alpha$) is the gain of the SAW amplifier, which can be found by combining Eqs. (11), (12), and (14) is

$$\alpha = k\,\text{Im}\left(\frac{\Delta k}{k}\right) = \frac{k}{2}\,\text{Im}\left(\frac{\Delta C}{C}\right) = \frac{k}{2}\,\text{Im}(\Delta C Z_a V_a) \tag{15}$$

In the following, ΔC and Z_a are to be derived. For a very thin semiconductor layer, a good approximation is to consider the charge layer infinitesimally thin. Thus, one-dimensional analysis, such as the model in Fig. 11.3.41*b*, can be employed.

In order to express ρ_s in terms of ϕ_{ah}, we start from the current equation and the continuity equation for the charge layer of the semiconductor:

$$\frac{\partial J_z}{\partial z} + \frac{\partial \rho}{\partial t} = 0 \qquad J_z = \sigma E_z - D_n \frac{\partial \rho}{\partial z} \tag{16}$$

where J_z = current density
$E_z = -\partial(\phi_a + \phi_c)/\partial z = jk(\phi_a + \phi_c)$ the electrical field
σ = conductivity of the semiconductor
D_n = diffusion coefficient of the electron carriers
ρ = bulk charge density
ϕ_c = potential induced by the charge layer. Then we have (at $y = h$)

$$\rho = \frac{-\phi_{ah}}{\dfrac{\phi_{ch}}{\rho} + \dfrac{D_n}{\sigma} + j\dfrac{V_a}{\sigma k}} \tag{17}$$

For a very thin semiconductor layer, ρ_s can be approximated with ρd (d is the thickness of the layer). The above equation leads to

$$\rho_s = \frac{-\phi_{ah}}{\dfrac{\phi_{ch}}{\rho_s} + \dfrac{1}{\sigma d}\left(D_n + j\dfrac{V_a}{k}\right)} \tag{18}$$

First, we need to find ϕ_{ch}/ρ_s. To simplify the analysis, we assume that the thin semiconductor layer is right on the piezoelectric substrate, i.e., $h \to 0$, and there is no encapsulation layer, $\epsilon_d \to \epsilon_0$. Then

$$\phi_{ch} = \begin{cases} Ae^{-ky}, & y \geq 0 \\ De^{ky}, & y < 0 \end{cases} \tag{19}$$

where the decay factor is k because the potential must satisfy the Laplace equation. With the following boundary conditions:

$$\begin{gathered} \phi_{ch}(y = 0^+) = \phi_{ch}(y = 0^-) \\ -\epsilon_0 \frac{\partial \phi_{ch}}{\partial y}(y = 0^+) + \epsilon_p \frac{\partial \phi_{ch}}{\partial y}(y = 0^-) = \rho_s \end{gathered} \tag{20}$$

Downloaded from Digital Engineering Library @ McGraw-Hill (www.digitalengineeringlibrary.com)
Copyright © 2004 The McGraw-Hill Companies. All rights reserved.
Any use is subject to the Terms of Use as given at the website.

RADIO-FREQUENCY AMPLIFIERS AND OSCILLATORS

we obtain

$$\frac{\phi_{ch}}{\rho_s} = \frac{1}{k(\epsilon_0 + \epsilon_p)} \tag{21}$$

Therefore,

$$\Delta C = -\frac{\rho_s W}{\phi_{ah}} = \frac{k(\epsilon_0 + \epsilon_p)W}{1 + \dfrac{(\epsilon_0 + \epsilon_p)}{\sigma d}(kD_n + jV_a)} \tag{22}$$

Now we proceed to find Z_a in terms of the electromechanical coupling coefficient K^2. By definition,

$$\begin{aligned} \frac{K^2}{2} &= \frac{\Delta k}{k}\bigg|_{\substack{\sigma=\infty \\ h=0}} = \frac{1}{2}\frac{\Delta C}{C}\bigg|_{\substack{\sigma=\infty \\ h=0}} = \frac{1}{2} Z_a V_a \Delta C\bigg|_{\substack{\sigma=\infty \\ h=0}} \\ &= \frac{1}{2}k(\epsilon_0 + \epsilon_p)WZ_a V_a = \frac{1}{2}(\epsilon_0 + \epsilon_p)W\omega Z_a \end{aligned} \tag{23}$$

Therefore,

$$Z_a = \frac{K^2}{(\epsilon_0 + \epsilon_p)W\omega} \tag{24}$$

Substituting Z_a and ΔC into Eq. (15)

$$\alpha = -\frac{K^2}{2}\frac{\dfrac{k\sigma d V_a}{\epsilon_0 + \epsilon_p}}{\left(\dfrac{k\sigma d}{\epsilon_0 + \epsilon_p} + kD_n\right)^2 + V_a^2} \tag{25}$$

Taking the applied electrical field E_0 into account, the current density in Eq. (16) and the charge density in Eq. (17) become

$$J_z = \sigma E_z + \rho\mu E_0 - D_n\frac{\partial \rho}{\partial z} \qquad \rho = \frac{-\phi_{ah}}{\dfrac{\phi_{ch}}{\rho} + \dfrac{D_n}{\sigma} + j\dfrac{V_a - \mu E_0}{\sigma k}} \tag{26}$$

where μE_0 gives the carrier drift velocity. It is clear that the gain is analogous to Eq. (25) except that the term V_a should be replaced with $V_a - \mu E_0$,

$$\alpha_{\mathrm{SAW}} = -\frac{K^2}{2}\frac{\dfrac{\sigma(dk)}{\epsilon_0 + \epsilon_p}(V_a - \mu E_0)}{(V_a - \mu E_0)^2 + \left[\dfrac{\sigma(dk)}{(\epsilon_0 + \epsilon_p)k} + kD_n\right]^2} \tag{27}$$

Downloaded from Digital Engineering Library @ McGraw-Hill (www.digitalengineeringlibrary.com)
Copyright © 2004 The McGraw-Hill Companies. All rights reserved.
Any use is subject to the Terms of Use as given at the website.

RADIO-FREQUENCY AMPLIFIERS AND OSCILLATORS

The gain for bulk acoustic wave amplifier can be expressed as

$$\alpha_{\text{BAW}} = -\frac{K^2}{2}\frac{\dfrac{\sigma}{\epsilon_p}(V_a - \mu E_0)}{(V_a - \mu E_0)^2 + \left(\dfrac{\sigma}{\epsilon_p k} + kD_n\right)^2} \tag{28}$$

Obviously, σ in the bulk wave amplifier has been replaced by $\sigma(kd)$ in the SAW amplifier because of the thin-film form semiconductor material.

In order to explain the approximate experimental linear relationship between gain and drift field illustrated by Fig. 11.3.39, the gain expression [Eq. (27)] can be further simplified. For InSb/$LiNbO_3$ SAW amplifier, σd is typically about 45×10^{-6}S/□, and $\epsilon_p = 50\epsilon_0 \approx 4.5 \times 10^{-12}$ F/cm, so that $\sigma d(\epsilon_0 + \epsilon_p) \gg kD_n$ and $V_0 - \mu E_0$. Thus, by dropping the negligible terms, we have

$$\alpha \approx \frac{K^2}{2}(\mu E_0 - V_a)\frac{\epsilon_p k}{\sigma d} \tag{29}$$

This is essentially the electronic gain equation given by Kotelyanski et al. (1978).

In the above derivation, we have assumed that $kd \ll 1$ and d is much smaller than the semiconductor's Debye length, which can be written as $(D_n\epsilon_s/\sigma)^{1/2} = 1/\zeta$. The assumptions imply that the potential and charge distribution inside the semiconductor is homogeneous along the y axis. To remove those restrictions and cover more general cases, the variation in y direction must be considered, i.e., analytical model Fig. 11.3.41*a* must be used.

A thicker semiconductor layer affects the SAW amplifier gain in two ways. First, the decay of acoustic potential in the semiconductor from the $y = h$ surface will become significant. The induced charge and the associated potential will decay accordingly, although at different rates. Therefore a field owing to the charge gradient in the y-direction will appear. The boundary condition now must be matched by the total potential from each side.

The second factor is the charge per unit area, which is needed in order to find ΔC. ρ_s is no longer ρd. It has to be calculated by the integration $\int \rho dy$.

The modification [see Lin (1995)] leads to

$$\alpha = -\frac{K^2}{2}\frac{\dfrac{\sigma \tanh(kd)(V_a - \mu E_0)}{\epsilon_h + \epsilon_p}\dfrac{e^{-2kh}}{F^2}}{\left[\dfrac{\sigma \tanh(kd)}{k(\epsilon_h + \epsilon_p)} + \zeta D_n \dfrac{\tanh(kd)}{\tanh(\zeta d)}\right]^2 + (V_a - \mu E_0)^2} \tag{30}$$

where

$$F = \frac{1}{2}\left[\left(\frac{\epsilon_d}{\epsilon_h} - 1\right)\frac{\epsilon_h - \epsilon_p}{\epsilon_h + \epsilon_p}e^{-2kh} + \left(\frac{\epsilon_d}{\epsilon_h} + 1\right)\right] \tag{31}$$

If $\epsilon_d = \epsilon_h$, $F = 1$.

Equation (55) is derived in Wang and Lin (1996). Equation (30) reduces to Eq. (27), when the semiconductor thickness d is extremely thin such that both $kd \ll 1$ and $\zeta d \ll 1$.

MAGNETIC AMPLIFIERS

Harold W. Lord

Static Magnetic Amplifiers

Static magnetic amplifiers can be divided into two classes, identified by the terms saturable reactor and self-saturating magnetic amplifier. A *saturable reactor* is an adjustable inductor in which the current-versus-voltage

Downloaded from Digital Engineering Library @ McGraw-Hill (www.digitalengineeringlibrary.com)
Copyright © 2004 The McGraw-Hill Companies. All rights reserved.
Any use is subject to the Terms of Use as given at the website.

RADIO-FREQUENCY AMPLIFIERS AND OSCILLATORS

relationship is adjusted by control magnetomotive forces applied to the core. A *magnetic amplifier* is a device using saturable reactors either alone or in combination with other circuit elements to secure amplification or control. A *simple magnetic amplifier* is a magnetic amplifier consisting only of saturable reactors. The abbreviation SR is used in this section to denote a *saturable reactor* and/or simple magnetic amplifier.

A self-saturating magnetic amplifier is a magnetic amplifier in which half-wave rectifying circuit elements are connected in series with the output windings of saturable reactors. It has been shown that saturable reactors can be considered to have negative feedback. Half-wave rectifiers in series with the load windings will block this intrinsic feedback. A self-saturating magnetic amplifier is therefore a parallel-connected saturable reactor with blocked intrinsic feedback. This latter term avoids the term self-saturation, which, although extensively used, does not have a sound physical basis. The abbreviation MA is used here to denote this type of high-performance magnetic amplifier.

Saturable-Reactor (SR) Amplifiers

The SR can be considered to have a very high impedance throughout one part (the *exciting interval*) of the half cycle of alternating supply voltage and to abruptly change to a low impedance throughout the remainder of the half cycle (the *saturation interval*). The phase angle at which the impedance changes is controlled by a direct current. This is the type of operation obtained when the core material of the SR has a highly rectangular hysteresis loop. Two types of operation, representing limiting cases, are discussed here, namely, *free even-harmonic currents* and *suppressed even-harmonic currents*. Intermediate cases are very complex, but use of one or the other of the two extremes is sufficiently accurate for most practical applications.

The present treatment is limited to resistive loads, the most usual type for SR applications. [See Storm (1955), for inductive dc loads and Wilson (1952), for inductive ac loads]. The basic principles of operation of SRs and MAs are given in more detail in Shea (1968).

Series-Connected SR Amplifiers

Basically, an SR circuit consists of the equivalent of two identical single-phase transformers. Figure 11.3.42 shows two transformers, SR_A and SR_B, interconnected to form a rudimentary series-connected SR circuit.

The two series-connected SR windings in series with the load are called *gate windings*, and the other two series-connected windings are called *control windings*. Note, from the dots that indicate relative polarity, that the gate windings are connected in series additive and the control windings are connected in series subtractive. By reason of these connections, the fundamental power frequency and all *odd* harmonics thereof will not appear across the total of the two control windings but any *even* harmonic induced in one control winding will be additive with respect to a corresponding even harmonic induced in the other control winding.

For this connection, SR_A and SR_B are normally so designed that each gate winding will accommodate one-half the alternating voltage of the supply without producing a peak flux density in the core that exceeds the knee of the magnetization curve, assuming no direct current is flowing in the control winding. Under these conditions, if SR_A is identical with SR_B, one-half of the supply voltage appears across each gate winding, and the net voltage induced in the control circuit is zero. The two SRs operate as transformers over the entire portion of each half cycle.

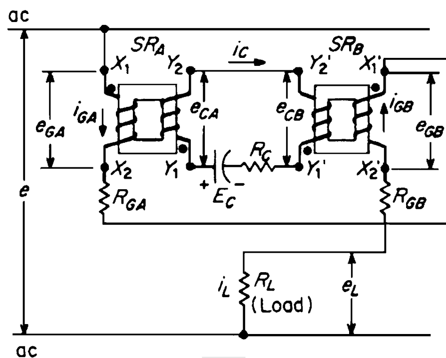

FIGURE 11.3.42 Series-connected SR amplifier.

When a direct current is supplied to the control circuit, each SR will have a saturation interval during a part of each cycle, SR_A during half cycles of one polarity and SR_B during half cycles of the opposite polarity. The ratio of the saturation interval to the exciting interval can be controlled by varying the direct current in the control winding.

When an SR core has a saturation interval during part of half cycles of one polarity, and there is a load or other impedance in series with the gate winding, even-harmonic voltages are induced in all other windings on that core. In the series connection, one SR gate winding can be the

Downloaded from Digital Engineering Library @ McGraw-Hill (www.digitalengineeringlibrary.com)
Copyright © 2004 The McGraw-Hill Companies. All rights reserved.
Any use is subject to the Terms of Use as given at the website.

RADIO-FREQUENCY AMPLIFIERS AND OSCILLATORS

series impedance for the SR, and large even-harmonic voltages will appear across the individual gate windings and control windings when direct current flows in the control windings. The amount of even-harmonic current which flows in the control circuit of Fig. 11.3.42 will depend on the impedance of the control circuit to the harmonic voltages. If the control-circuit impedance between terminals Y_1 and Y_1' is low with respect to the induced harmonic voltages of the control windings (usually referred to as a *relatively low* control-circuit impedance), the harmonic currents can flow freely in this circuit, and the SR circuit is identified by the term *free even-harmonic currents*. If the control-circuit impedance is high with respect to the induced harmonic voltages (a *relatively high* control-circuit impedance), the harmonic-current flow is suppressed and the SR circuit is identified by the term *suppressed even-harmonic currents*.

If R_C in Fig. 11.3.42 is relatively low and the source impedance of the dc control current is low, the circuit is of the free even-harmonic-currents type and the two SRs are tightly coupled together by the control circuit. If one SR is in its saturation interval, it will reflect a low impedance to the gate winding of the other SR, even though it is then operating in its exciting interval. Thus, during the saturation interval of any core, transformer action causes both gate windings to have low impedances and current can flow from the ac source to the load, with correspondingly high harmonic circulating currents in the control circuit. When both cores are in their exciting intervals, only the low core-exciting current can flow and the current circulating in the control circuit is substantially zero.

If the exciting current is so low as to be negligible, and if N_G are the turns in each gate winding, N_C are the turns in each control winding, I_G is the rectified average of the load current, and I_C is the average value of the control current, then applying the law of equal ampere-turns for transformers provides the following expression for the circuit in Fig. 11.3.42: $I_C N_C = I_G N_G$. This is the law of equal ampere-turns for the series-connected SR with resistive load. It applies to operation in the so-called *proportional region*, the upper limit of this region being that point in the control characteristic where the load current is limited solely by the load circuit resistance. Figure 11.3.43 shows the gate-current circuit and control-circuit current at one operating point in the proportional region. An increase in control current causes a decrease in the angle α, thereby increasing I_L, the rectified average of the current to the load.

Parallel-Connected SR Amplifiers

Figure 11.3.44 shows the circuit diagram for the parallel-connected SR. Each gate winding is connected directly between the ac supply and the load resistance, thus providing two parallel paths through the SR. There is therefore a low-impedance path for the free flow of even-harmonic currents, even though the impedance of the control circuit happens to be relatively high. As a result, the parallel-connected SR is always of the *free flow of even-harmonic-currents* type, the cores operate in the same manner as described in the previous paragraph, and the waveshapes of currents to the *load* are as shown in Fig. 11.3.43. However, the gate winding currents are different, as shown in Fig. 11.3.45.

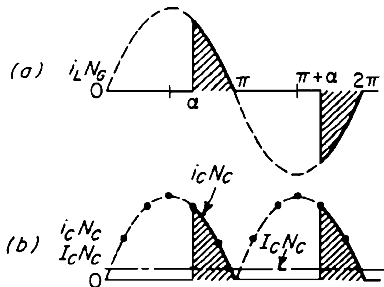

FIGURE 11.3.43 Currents in circuit of Fig. 11.3.42, for free even-harmonic-current conditions: (*a*) gate current; (*b*) control-circuit current.

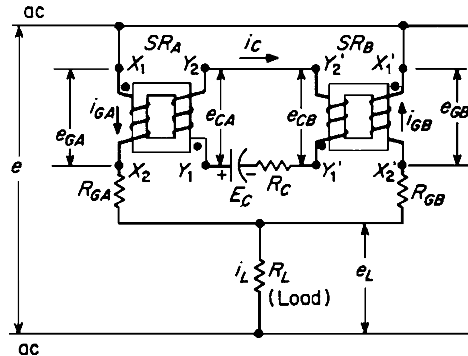

FIGURE 11.3.44 Parallel-connected SR amplifier.

Downloaded from Digital Engineering Library @ McGraw-Hill (www.digitalengineeringlibrary.com)
Copyright © 2004 The McGraw-Hill Companies. All rights reserved.
Any use is subject to the Terms of Use as given at the website.

RADIO-FREQUENCY AMPLIFIERS AND OSCILLATORS

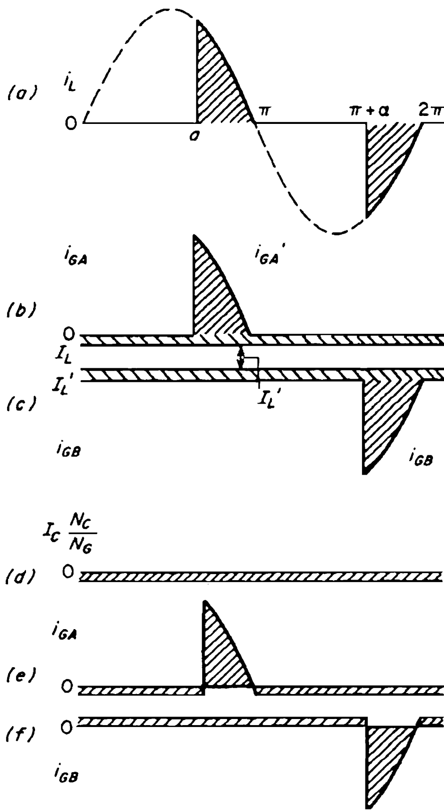

FIGURE 11.3.45 Currents in the circuit of Fig. 11.3.44 for free even-harmonic-current conditions: (*a*) load current; (*b*) components of load current in SR_A gate winding; (*c*) same in SR_B; (*d*) control-circuit current; (*e*) gate-current in SR_A; (*f*) same in SR_B.

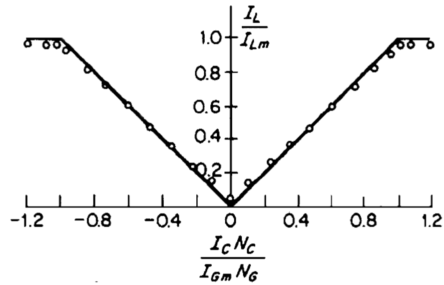

FIGURE 11.3.46 Control characteristic of SR amplifier applying both to free and suppressed even-harmonic conditions.

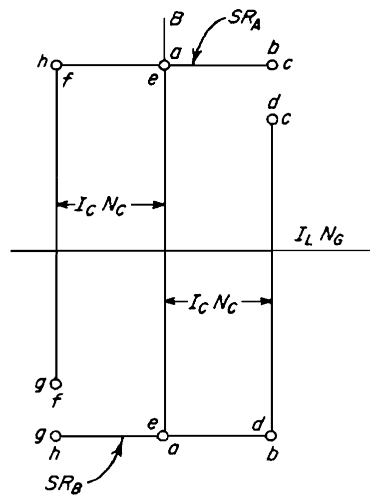

FIGURE 11.3.47 Idealized operating hysteresis loops for suppressed even-harmonic-current condition.

It is obvious from Fig. 11.3.45 that $I_L' = -I_L/2$. Since, except for the low-excitation requirements for the core, the net ampere-turns acting on the core must be zero during the exciting interval, then $I_L'N_G + I_C N_C = 0$. Using the above equation to eliminate I_L', the result is $I_C N_C = I_L N_G/2$. Figure 11.3.46 shows the control characteristic of saturable core amplifiers applicable both to free and suppressed even-harmonic modes of operation.

Series-Connected SR Circuit with Suppressed Even Harmonics

This circuit is usually analyzed by assuming operation into a short circuit and the control *current* from a current source. Figure 11.3.47 shows idealized operating minor hysteresis loops for this circuit, and Fig. 11.3.48 shows pertinent current and voltage waveshapes lettered to correspond to Fig. 11.3.47. Note that this current supplies a square wave of current to the load so long as it is operating in the proportional region. Energy is interchanged between the power-supply circuit and the control circuit so as to accomplish this type of operation. If a large inductor is used to maintain substantially ripple-free current in the control circuit, the energy

Downloaded from Digital Engineering Library @ McGraw-Hill (www.digitalengineeringlibrary.com)
Copyright © 2004 The McGraw-Hill Companies. All rights reserved.
Any use is subject to the Terms of Use as given at the website.

RADIO-FREQUENCY AMPLIFIERS AND OSCILLATORS

interchanged between the supply voltage and control circuit is alternately stored in, and given up by, the control-circuit inductor.

Gain and Speed of Response of SRs

It is obvious from the generalized control characteristic that the current gain is directly proportional to the ratio of the control winding turns to the gate winding turns. Thus $I_L/I_C = N_C/N_G$. If R_C is the control-circuit resistance and R_L is the load resistance, the power gain GP is $N_C^2R_L^2/N_G^2R_C^2$.

The response time of saturable reactors is the combination of the time constants of the control circuit and of the gate-winding circuit. Expressed in terms of the number of cycles of the supply frequency, the time constant of the control winding of a series-connected SR is $\tau_C = R_0N_C^2/4R_CN_C^2$ cycles. If the SR is operating underexcited, a transportation lag may cause an additional delay in response.

High-Performance Magnetic Amplifier (MA)

If a rectifier is placed in series with each gate winding of a parallel-connected SR and the rectifiers are poled to provide an ac output, it becomes a type of high-gain MA circuit called the *doubler circuit*. When this is done, the law of equal ampere-turns no longer applies, and the transfer characteristic is mainly determined by the magnetic properties of the SR cores. The design of an MA therefore requires more core-materials data than are required for SRs in simple magnetic amplifier circuits. The text of this section assumes that the designer has the required magnetic-core-materials data on hand, since such data are readily available from the manufacturers of cores for use in high-performance MAs.

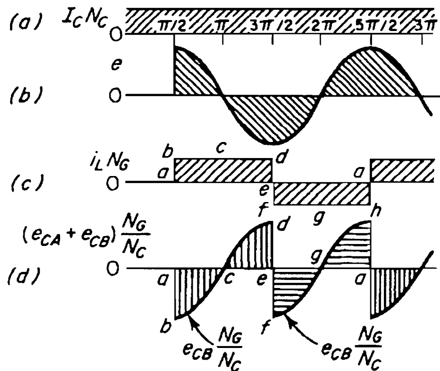

FIGURE 11.3.48 Series-connected suppressed even-harmonic condition: (*a*) control-circuit current; (*b*) applied input voltage; (*c*) gate winding and load current; (*d*) voltage across series-connected control coils.

Descriptions of the operation of MAs require several terms which are defined here for reference.

Firing. In a magnetic amplifier, the transition from the unsaturated to the saturated state of the saturable reactor during the conducting or gating alternation. Firing is also used as an adjective modifying phase or time to designate when the firing occurs.

Gate angle (firing angle). The angle at which the gate impedance changes from a high to a low value.

Gating. The function or operation of a saturable reactor or magnetic amplifier that causes it, during the first portion of the conducting alternation of the ac supply voltage, to block substantially all the supply voltage from the load and during a later portion allows substantially all the supply voltage to appear across the load. The "gate" is said to be virtually closed before firing and substantially open after firing.

Reset, degree of. The reset flux level expressed as a percentage or fraction of the reset flux level required to just prevent firing of the reactor in the subsequent gating alternation under given conditions.

Reset flux level. The difference in saturable-reactor core flux level between the saturation level and the level attained at the end of the resetting alternation.

Resetting (presetting). The action of changing saturable-reactor core flux level to a controlled ultimate reset level, which determines the gating action of the reactor during the subsequent gating alternation. The terms resetting and presetting are synonymous in common usage.

Resetting half cycle. The half cycle of the MA ac supply voltage at which resetting of the saturable reactor may take place.

Downloaded from Digital Engineering Library @ McGraw-Hill (www.digitalengineeringlibrary.com)
Copyright © 2004 The McGraw-Hill Companies. All rights reserved.
Any use is subject to the Terms of Use as given at the website.

RADIO-FREQUENCY AMPLIFIERS AND OSCILLATORS

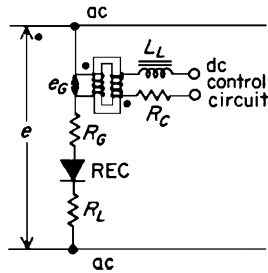

FIGURE 11.3.49 Half-wave MA circuit.

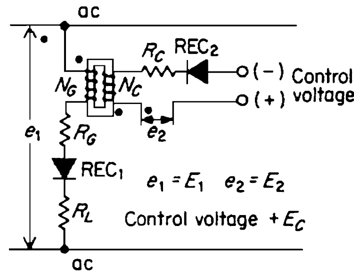

FIGURE 11.3.50 Voltage-controlled MA circuit.

Half-Wave MA Circuits

Figure 11.3.49 shows a half-wave MA circuit with control from a source of controllable direct *current*. Figure 11.3.50 shows a half-wave MA circuit with control from a controllable source of direct *voltage*. The following sequence of operation is the same for both circuits and is described in connection with Fig. 11.3.51.

1. During the gating half cycle (diode REC or REC_1 conducting) the core flux increases toward a saturation level (3′) from some reset flux level (0) and the current to the load R_L is very low.
2. When saturation of the SR occurs at 2′, firing occurs and current flows to the load for the rest of the gating half cycle, leaving the core flux at 4′.
3. During the resetting half cycle (diode REC or REC_1 blocking) the SR core is reset from 4′ through 5′ to a value of reset flux level corresponding to *B*′ and 0.

The waveshape of the current to the load is the same for both circuits, being a portion of one polarity of sine wave (phase-controlled half-wave). The two types of control circuits differ as follows:

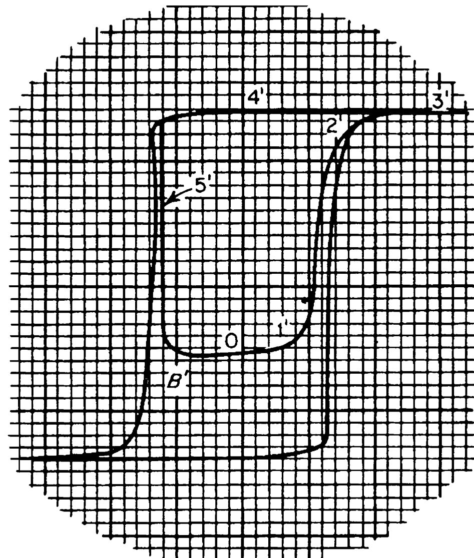

FIGURE 11.3.51 Major and operating minor dynamic hysteresis loops for circuit of Fig. 11.3.49.

1. The curve on the reset portion of the hysteresis loop between 4′ and 0 is as shown in Fig. 11.3.51 for the current control type of control circuit (Fig. 11.3.49), but for the circuit of Fig. 11.3.50, the resetting portion of the curve in the region 5′ is not a vertical line and may coincide with the outer major hysteresis loop for a substantial portion of the resetting period.
2. The output of the circuit of Fig. 11.3.49 is a maximum for zero dc control current, but for Fig. 11.3.50 the output is a minimum for zero dc control voltage.

The operation of a half-wave MA can be summarized as follows: (1) During the gating half cycle, the core acts to withhold current from the load for a portion of each half cycle, the length of the withholding period being determined by the degree of reset of core flux provided during the immediately preceding resetting half cycle. (2) During the resetting half cycle, the degree of reset can be controlled by varying the amount of direct current of proper polarity in the control winding, or by varying the amount of average voltage of proper polarity applied to the control winding. (3) The amount of current and power required to reset the core is primarily a function of the excitation requirements of the core and bears no direct relationship to the power delivered to the load.

Downloaded from Digital Engineering Library @ McGraw-Hill (www.digitalengineeringlibrary.com)
Copyright © 2004 The McGraw-Hill Companies. All rights reserved.
Any use is subject to the Terms of Use as given at the website.

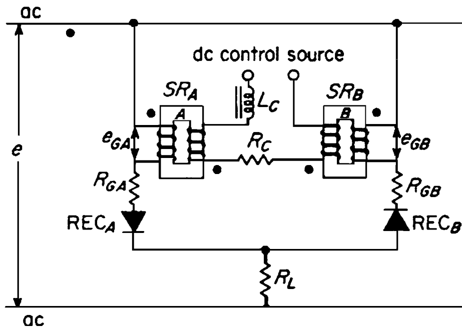

FIGURE 11.3.52 Full-wave ac-output MA circuit with high-impedance control circuit.

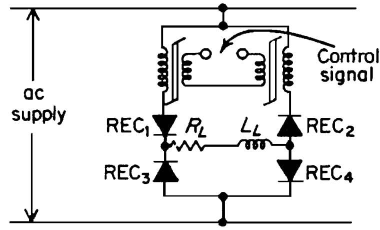

FIGURE 11.3.53 Full-wave bridge MA circuit with inductive load.

Full-Wave MA Circuits

Two half-wave MA circuits can be combined to provide either full-wave ac output (Fig. 11.3.52) or full-wave dc output (Fig. 11.3.53). During the gating half cycle, all gate windings act in the same manner as described for the half-wave MA circuit. Because of an interaction of the common load resistor voltage with the availability of inverse voltage across a rectifier during its resetting half cycle, each half-wave part of Fig. 11.3.52 cannot be assumed to operate independently of its mate. The differences in control characteristics are shown by Fig. 11.3.54, where curve *A* applies to the circuit of Fig. 11.3.49 and curve *B* applies to the circuit of Fig. 11.3.52.

Equations for MA Design

For SRs in simple MA circuits, since the ampere-turn balance rules apply, their design is so similar to transformer design that ordinary transformer design procedures are applicable. For SRs in MA circuits, the gate windings must carry rms load currents that are related to the ac and dc load currents in the same manner that rectifier transformer secondary rms currents are related to the load current. Gate windings must be able to withstand a full half cycle of ac supply voltage, without saturation, for a total flux swing from $-B\mu_m$ to $+B\mu_m$, where $B\mu_m$ is the flux density at which the permeability of the core material is a maximum. In the cgs system of units:

Maximum ac supply voltage, rms: $E_e = 4.44 N_G B\mu_m A f \times 10^{-8}$, where N_G is gate winding turns, A is core area, and f is supply frequency.

Maximum load current for firing angle $\alpha = 0°$ (rectified average): $I_{LM} = E_e/1.11(R_G + R_L)$, where R_G is total gate winding resistance, including diode drops, and R_L is the effective load resistance.

For current-controlled MA circuits the following equations apply:

Minimum load current ($\alpha = 180°$); $I_{LX} = 2I_X = 2H_{csf}l/0.4\pi N_G$, where I_X = exciting current (A) of one SR core. H_{csf} = sine flux coercive force of the core material (Oe) and l = mean length of magnetic circuit of one core.

Control current for upper end of control current: $I_C = H_C l/0.4\pi N_C$, where H_C = dc coercive force of the core material.

Control current for minimum load-current point: $I_C = H_{csf} l/0.4\pi N_C$. Ampere-turn gain $G_{AT} = (I_{LM}/2I_X)\pi$.

Time constant $\tau_C = 0.9\pi E_e R N_C^2/4 f I_x R_C N_G^2$ seconds, where R_C is the control circuit resistance and assuming $\alpha = 90°$. This equation does not take into account a transportation or any underexcited effects which increase the delay time.

Power gain $G_p = G_{AT}^2 (N_C/N_G)^2 (R_L/R_C)$, where k_f = form factor (ratio of rms to average values). If only average values are used, k_f is unity. At $\alpha = 90°$, dynamic power gain $G_D = G_p/\tau_C = \pi f I_{LM} R_L / I_X (R_G + R_L)$ per second.

Downloaded from Digital Engineering Library @ McGraw-Hill (www.digitalengineeringlibrary.com)
Copyright © 2004 The McGraw-Hill Companies. All rights reserved.
Any use is subject to the Terms of Use as given at the website.

RADIO-FREQUENCY AMPLIFIERS AND OSCILLATORS

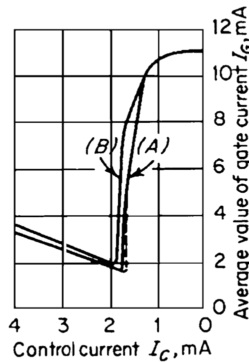

FIGURE 11.3.54 MA circuit control characteristics: (A) half-wave circuit; (B) full-wave ac-output circuit.

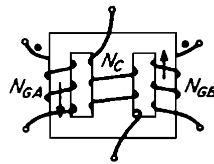

FIGURE 11.3.55 Three-legged SR core-and-coil configuration.

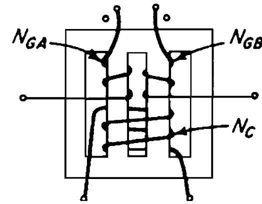

FIGURE 11.3.56 Four-legged SR core-and-coil configuration.

For voltage-controlled MA circuits, the following equations apply to Fig. 11.3.50:

AC bias voltage $E_2 > E_1N_C/N_G$ and of indicated relative polarities. A value of $E_2 = 1.2E_1N_C/N_G$ is usually adequate. Since the dc control voltage E_C acts to inhibit the resetting effect of E_2, a firing angle $\alpha = 0°$ occurs when $E_C \geq \sqrt{2E_2}$.

A single-stage amplifier has a half-cycle transport lag and no other time delay unless the resetting is inhibited by common-load interactions with other half-wave-amplifier elements.

Maximum average load current $I_{LM} = 0.9E_1/(R_G + R_L)$.

Minimum average load current $I_{LX} = I_X = H_{csf}\,l/0.4\pi N_G$.

The calculation of the power gain of voltage-controlled MA circuits largely depends on the control circuit. The dc control voltage of Fig. 11.3.50 actually must *absorb* power from the ac bias circuit during much of its control range. Assuming that $E_2 = 1.2E_1N_C/N_G$ and a resistor R'_C is connected across the control source, which has a drop of $0.2E_2$ at cutoff, then $R'_C = 0.24E_1N_C^2/N_{GX}^2$. The maximum dc control voltage is then $1.2\sqrt{2}\ E_1 N_C/N_G$.

When the dc control voltage, $E_C > 2E_2$, rectifier REC_2 is blocking all the time, and so the only load on the control source is R'_C. Therefore the maximum power from the control source $P_C = E_C^2 / R_C^1 = 5\sqrt{2E_1I_X}$.

The maximum power output is $P_0 = I_{LM}^2R_L(0.9E_1)^2/(R_G + R_L)^2$.

The power gain is then $G_p = P_0/P_C$ if the gain is assumed to be linear over most of the control characteristic. This can also be written $G_p = I_{LM}^2G_p - I_{LM}^2R_L/5\sqrt{2E_1I_X}$.

Core Configurations

Figures 11.3.55 and 11.3.56 show two coil-and-core configurations commonly used for SRs. The best core-and-coil geometry for the SRs and MAs is the toroid-shaped core with the gate winding uniformly wound over the full 360° of the core. Full-wave operation requires two such cores. After winding a gate winding on each core of a matched pair, the two cores and coils can be stacked together coaxially and the required control coils wound over the stack. The gate coils are so connected into the load circuit that no fundamental or odd-harmonic voltage is induced in the control windings.

Downloaded from Digital Engineering Library @ McGraw-Hill (www.digitalengineeringlibrary.com)
Copyright © 2004 The McGraw-Hill Companies. All rights reserved.
Any use is subject to the Terms of Use as given at the website.